Fate of terrigenous organic matter across the Laptev Sea from the mouth of the Lena River to the deep sea of the Arctic interior

Lisa Bröder [a,b*], Tommaso Tesi [a,b,c], Joan A. Salvadó [a,b], Igor P. Semiletov [d,e,f], Oleg V. Dudarev [e,f], Örjan Gustafsson [a,b]

[a] *Department of Environmental Science and Analytical Chemistry, Stockholm University, Stockholm, Sweden*

[b] *Bolin Centre for Climate Research, Stockholm University, Stockholm, Sweden*

[c] *Institute of Marine Sciences – National Research Council, Bologna, Italy*

[d] *International Arctic Research Center, University Alaska Fairbanks, Fairbanks, USA*

[e] *Pacific Oceanological Institute, Russian Academy of Sciences, Vladivostok, Russia*

[f] *Tomsk National Research Politechnical University, Tomsk, Russia*

*corresponding author: lisa.broder@aces.su.se

14 **Abstract**

15 Ongoing global warming in high latitudes may cause an increasing supply of permafrost-

16 derived organic carbon through both river discharge and coastal erosion to the Arctic

17 shelves. Mobilized permafrost carbon can be either buried in sediments, transported to the

18 deep sea or degraded to CO_2 and outgassed, potentially constituting a positive feedback to

19 climate change.

20 This study aims to assess the fate of terrestrial organic carbon (TerrOC) in the Arctic marine

21 environment by exploring how it changes in concentration, composition and degradation

22 status across the wide Laptev Sea shelf. We analyzed a suite of terrestrial biomarkers as

23 well as source-diagnostic bulk carbon isotopes ($\delta^{13}C$, $\Delta^{14}C$) in surface sediments from a

24 Laptev Sea transect spanning more than 800 km from the Lena River mouth (< 10 m water

25 depth) across the shelf to the slope and rise (2000-3000 m water depth). These data provide

26 a broad view on different TerrOC pools and their behavior during cross-shelf transport. The

27 concentrations of lignin phenols, cutin acids and high-molecular weight (HMW) wax lipids

28 (tracers of vascular plants) decrease by 89-99 % along the transect. Molecular-based

29 degradation proxies for TerrOC (e.g., the carbon preference index of HMW lipids, the HMW

30 acids/alkanes ratio and the acid/aldehyde ratio of lignin phenols) display a trend to more

31 degraded TerrOC with increasing distance from the coast. We infer that the degree of

32 degradation of permafrost-derived TerrOC is a function of the time spent under oxic

33 conditions during protracted cross-shelf transport. Future work should therefore seek to

34 constrain cross-shelf transport times in order to compute a TerrOC degradation rate and

35 thereby help to quantify potential carbon-climate feedbacks.

1 Introduction

Amplified global warming in high latitudes has raised growing concern about potential positive carbon-climate feedbacks. Arctic soils store about half of the global soil organic carbon (Tarnocai et al., 2009), with 60 % of this in perennially frozen grounds (Hugelius et al., 2014). With ongoing climate change these vast carbon reservoirs become increasingly vulnerable. Mobilization and transport of old terrigenous organic carbon (TerrOC) into the Arctic Ocean is expected to intensify (Gustafsson et al., 2011) through enhancing river discharge (McClelland et al., 2008) with augmenting sediment loads (Gordeev, 2006; Syvitski, 2002) and accelerating coastal erosion (Günther et al., 2013). This material can be buried in the sediments of the Arctic shelves, transported across the margin towards deeper basins or degraded and re-introduced into the modern carbon cycle as CO_2, thereby not only providing a potential positive feedback to global warming, but also causing severe ocean acidification (Semiletov et al., 2016). The fate of permafrost-released TerrOC in the marine environment is thus crucial for future climate projections, yet insufficiently understood (Vonk and Gustafsson, 2013).

The East Siberian Arctic Shelf (ESAS) is with a width of > 800 km the world's largest continental shelf. It receives TerrOC both from the erosion of the East Siberian shoreline, largely consisting of organic-rich, late-Pleistocene ice-complex deposits (Yedoma), and via the Great Russian Arctic Rivers, which drain extensive areas of continuous and discontinuous permafrost. The Laptev Sea is a representative for the TerrOC dominated Siberian shelf seas, since its main organic carbon input originates from substantial coastal erosion (as observed in the Buor-Khaya Bay, Sánchez-García et al., 2011; Semiletov et al., 2011; Vonk et al., 2012) and the Lena River, the main fluvial sediment source for the entire ESAS (Holmes et al., 2002).

Previous studies have focused on near-shore areas and the inner shelf (e.g. Bröder et al., 2016; Charkin et al., 2011; Feng et al., 2015; Karlsson et al., 2011; Salvadó et al., 2015; Sánchez-García et al., 2011; Semiletov et al., 2005, 2012, 2013; Tesi et al., 2014; Vonk et al., 2010, 2012, 2014; Winterfeld et al., 2015b, 2015a). They reported large fractions of old

64   TerrOC in particulate organic carbon (POC) and surface sediments close to the coast, using

65   different approaches such as applying carbon-isotope-based source apportionment (e.g.

66   Gustafsson et al., 2011; Semiletov et al., 2005; Vonk et al., 2010, 2012, 2014; Salvadó et al.,

67   2015, for the iron-associated OC fraction in the sediment) and by analyzing terrigenous

68   biomarkers in both surface sediments (e.g. Feng et al., 2013; Stein and Macdonald, 2004;

69   Tesi et al., 2014, 2016) and POC in the water column (e.g. Charkin et al., 2011; Karlsson et

70   al., 2011; Winterfeld et al., 2015a). This is the first study that encompasses sampling stations

71   along the entire transect from the Lena River mouth, across the wide Laptev Sea shelf, to the

72   continental slope and rise. Our major objective was to gain new insights regarding the

73   behavior of different TerrOC pools, in particular investigating potential degradation of

74   permafrost-released material along the land-shelf-basin continuum. The Laptev Sea and

75   adjacent East Siberian Sea are among the widest continental margins on Earth (Jakobsson

76   et al., 2004). Protracted cross-shelf transport may hence result in long oxygen exposure

77   times, which might exert first order control on TerrOC degradation (e.g. Keil et al., 2004). Our

78   study area is thus well suited to test hypotheses on the fate of permafrost carbon in terms of

79   carbon-climate feedback. We have therefore characterized TerrOC in surface sediments

80   along the Laptev Sea transect on both bulk and molecular level, exploiting source-diagnostic

81   bulk carbon isotopes (δ^{13}C, Δ^{14}C) as well as an extensive biomarker suite (lignin phenols and

82   cutin acids obtained by alkaline CuO oxidation and high-molecular-weight solvent-extractable

83   lipids, such as *n*-alkanes and *n*-alkanoic acids).

2 Material and Methods

2.1 Study area

The Laptev Sea is the shallowest of the Arctic shelf seas with an average depth of 48 m (Jakobsson et al., 2004). It spans over 498,000 km^2 with a volume of 24,000 km^3 and is located between the Kara Sea and Severnaya Zemlya in the West and the East Siberian Sea and the New Siberian Islands in the East. The main sources of particulate organic carbon (POC) for the Laptev Sea are terrigenous, both from coastal erosion and river runoff (Sánchez-García et al., 2011; Stein and Macdonald, 2004). Marine primary production is limited to on average two ice-free months per year and therefore generally low. Nutrient-poor waters on the Siberian shelves resulting from a strong stratification further impede phytoplankton growth (Sakshaug, 2004).

The destabilization of Pleistocene Ice-Complex Deposits along the coastline is a main sediment source for the Laptev Sea (Rachold et al., 2000). The total POC input from coastal erosion to Laptev and East Siberian Sea is estimated to be between 4.0 Tg yr^{-1} (Semiletov, 1999; Stein and Fahl, 2000) and 22 ± 8 Tg yr^{-1} (including net subsea permafrost-carbon erosion, Vonk et al., 2012).

The Lena River is estimated to provide 20.7 Tg of sediment per year (Holmes et al., 2002), i.e. > 70 % of the total riverine input to the Laptev Sea (Gordeev, 2006)with an average water discharge of 588 km^3 yr^{-1} (Holmes et al., 2012). It drains a watershed of ~2.46 x 10^6 km^2 (Holmes et al., 2012), of which 77 % is underlain by continuous permafrost (Amon et al., 2012). Water discharge peaks in June, during the spring flood, when about 75 % of total organic carbon is delivered (Rachold et al., 2004). Total POC discharge by the Lena River can be up to 0.38 Tg yr^{-1} (Semiletov et al., 2011).

Sediment transport pathways are largely influenced by the prevailing atmospheric conditions: During cyclonic summers (i.e. positive phase of the Arctic Oscillation), northerly winds predominate, strengthening the Siberian Coastal Current, which transports Lena River water masses along the coast towards the East Siberian Sea; whereas during anticyclonic summers (i.e. negative phase of the Arctic Oscillation and mainly southerly winds) the Lena

112   River plume is exported onto the mid-shelf and towards the deep part of the Arctic Ocean

113   (Charkin et al., 2011; Dmitrenko et al., 2008; Guay et al., 2001; Wegner et al., 2013;

114   Weingartner et al., 1999). Sediment transport in the Laptev Sea is strongly seasonal. The

115   main transport of Lena River water with high concentrations of suspended particulate matter

116   (SPM) towards the mid-shelf takes place shortly after river-ice breakup (Wegner et al., 2005).

117   During the ice-free summer, SPM circulates between inner and mid-shelf with very little

118   material escaping over the shelf break to the deeper parts of the Arctic Ocean. Significant

119   sediment export is suggested to happen during freeze-up through SPM that is incorporated

120   in sea ice and then transported across the continental margin (Dethleff, 2005; Eicken et al.,

121   1997) or through the formation of dense bottom water resulting from brine ejection (Dethleff,

122   2010; Ivanov and Golovin, 2007). Hardly any sediment transport occurs beneath the ice

123   cover.

124   Holocene-scale linear sedimentation rates for the Laptev Sea vary between 0.12 and 0.59

125   mm yr^{-1} according to ^{14}C dating of marine bivalves (Stein and Fahl, 2004, and citations

126   therein), whereas centennial-scale ^{210}Pb-derived rates for the more recent Laptev Sea can

127   be up to 1.3 mm yr^{-1} (Vonk et al., 2012). These rates do not seem to be correlated with water

128   depth on the shelf, but values for the continental slope and rise tend to be on the lower end

129   (0.12-0.38 mm yr^{-1}) (Stein and Fahl, 2004, and citations therein).

130

131   2.2 Sampling

132   Sediment sampling locations span from close to the Lena River mouth and in the Buor-

133   Khaya Bay, across the shelf, to the continental slope and rise, covering a transect of > 800

134   km with water depths increasing by more than two orders of magnitude. Samples SW-1, SW-

135   2, SW-3, SW-4, SW-6, SW-14, SW-23 and SW-24 were collected during the SWERUS-C3

136   expedition on IB *ODEN* during summer 2014 using an Oktopus multicorer (8 Plexiglas tubes,

137   10 cm diameter). All other samples were collected during the International Siberian Shelf

138   Study (ISSS-08) expedition onboard the RV *Yacob Smirnitskyi* during summer 2008. The

139   YS-4, YS-6, YS-13 and YS-14 samples were taken with a GEMAX gravity corer (2 Plexiglas

140   tubes, 9 cm diameter); YS-9 and TB-46 were collected with a Van Veen grab sampler. For

141   the grab samples only surface sediments (uppermost cm) were subsampled and used in this

142   study. Sediment cores were cut into 1 cm slices within 24 hours after sampling. To account

143   for lower sediment accumulation rates on the rise, for SW-1, SW-2, SW-3 and SW-4 a higher

144   resolution of 0.5 cm for the top 10 cm was chosen. The depositional age for all samples is

145   thus between ~8 and ~70 years (depending on which sedimentation rates are employed). All

146   samples were kept frozen throughout the expedition and freeze-dried upon arrival to

147   Stockholm University laboratories. See Semiletov and Gustafsson (2009) for more

148   information on the ISSS-08 expedition. For exact sampling locations see Table 1.

149

150   2.3 Surface area

151   All surface area analyses have been performed on a Micromeritics Gemini VII Surface Area

152   and Porosity analyzer. Freeze-dried subsamples of ~0.7 g were furnaced at 400 °C for 12 h

153   and gently cooled down to room temperature to remove all organic material. Keil and Cowie

154   (1999) have shown that this method yields statistically similar results to the method using

155   removal with sodium pyrophosphate/ hydrogen peroxide (Mayer, 1994). The samples were

156   then desalted by repeated mixing with 50 ml of MilliQ water and centrifugation (20 min at

157   8000 rpm), followed by further freeze-drying. Directly prior to analysis they were degassed in

158   a Micromeritics FlowPrep 060 Sample Degas System for 2 h at 200 °C under a constant

159   nitrogen flow. Each analysis was initiated by measuring the free space in the vial. The

160   specific surface areas were derived from 6 pressure-point measurements (relative pressure

161   p/p0 = 0.05-0.3, equilibration time 5 s) with nitrogen as adsorbing gas (Brunauer et al., 1938).

162   The instrumental precision was 0.1-0.3 m^2 g^{-1}, which corresponds to a relative uncertainty of

163   about 1 %. The performance of the instrument was monitored with the surface area

164   reference material Carbon Black (21.0 ± 0.75 m^2 g^{-1}) provided by Micromeritics.

165

166   2.4 X-Ray Fluorescence

167 The mineral composition of ~1 g freeze-dried, homogenized subsamples was also

168 characterized with a wavelength dispersive sequential Philips PW2400 X-ray Fluorescence

169 (XRF) spectrometer. Prior to the analysis, sediment samples were combusted for 12h at 450

170 °C to remove the organic fraction. The XRF was operated under vacuum conditions on

171 samples prepared as glass beads using lithium tetraborate and melted with a fluxer Claisse

172 Fluxy (~1150°C) (Mercone et al., 2001). The relative error was less than 0.6 % for major

173 elements and less than 3 % for trace elements. In this study only SiO_2, Al_2O_3 and CaO are

174 reported.

175

176 2.5 Bulk elemental and carbon isotope analysis

177 Concentration and $\delta^{13}C$ isotopic composition of total organic carbon (TOC) were determined

178 at the Stable Isotope Laboratory, Department of Geological Sciences, Stockholm University.

179 Homogenized subsamples of ~10 mg were repeatedly acidified (HCl,1.5 M, Ag capsules) to

180 remove carbonates (Nieuwenhuize et al., 1994). TOC concentrations and $\delta^{13}C$ isotopic

181 composition were measured simultaneously with a Carlo Erba NC2500 elemental analyzer

182 connected via a split interface to a Finnigan MAT Delta V mass spectrometer. TOC

183 concentrations were blank corrected and the relative error was < 1 %. Stable isotope data

184 are reported relative to VPDB using the $\delta^{13}C$ notation.

185 Radiocarbon analyses of acidified samples were conducted at the US National Ocean

186 Sciences Accelerator Mass Spectrometry (NOSAMS) Facility of the Woods Hole

187 Oceanographic Institution, USA, according to their standard routines (Pearson et al., 1998).

188 The relative error of the measurements was < 0.5 %. Radiocarbon data are reported using

189 the $\Delta^{14}C$ notation following Stuvier and Polach (1977).

190

191 2.6 Biomarkers

192 2.6.1 CuO-oxidation products

193 Microwave-assisted alkaline CuO oxidation was performed according to the method

194 established by Goñi and Montgomery (2000). Homogenized subsamples of 100-400 mg of

195   sediment (corresponding to 2-5 mg OC) were combined with 300 mg of copper(II) oxide and

196   50 mg of ferrous ammonium sulfate and oxidized under oxygen-free conditions (degassed

197   NaOH, 8 wt %) at 150 °C for 90 min using an UltraWAVE Milestone 215 Microwave oven.

198   After oxidation, known amounts of trans-cinnamic acid and ethyl vanillin were added as

199   recovery standards. Samples were acidified to pH 1 with HCl (12 M) and repeatedly

200   extracted with ethyl acetate. Anhydrous Na_2SO_4 was added to remove remaining water. The

201   solvent was evaporated and extracts re-dissolved in pyridine. For quantification, subsamples

202   were derivatized with bis-trimethylsilyl-trifluoroacetamide (BSTFA) + 1 %

203   trimethylchlorosilane (TMCS) and analyzed on a gas-chromatograph mass spectrometer in

204   full scan mode (GC-MS, Agilent) using a DB5-MS capillary column (60 m x 250 μm, 0.25 μm

205   stationary phase thickness, Agilent J&W) with a temperature profile of initially 60 °C followed

206   by a ramp of 5 °C min^{-1} until reaching and holding 300 °C for 5 min. The quantification of

207   lignin phenols, benzoic acids, and p-hydroxybenzenes was achieved by comparison to the

208   response factors (key ions) of commercially available standards. For cutin-derived products,

209   fatty acids and dicarboxylic acids the response factor of trans-cinnamic acid was used as in

210   Goñi et al. (1998).

211

212   2.6.2 Solvent-extractable lipids

213   Wax lipids were extracted by means of accelerated solvent extraction (Dionex ASE 300)

214   using dichloromethane:methanol (9:1) according to the method described by Wiesenberg et

215   al. (2004). Pre-rinsed stainless-steel vessels were loaded with ~3 g of freeze-dried sediment,

216   filled up with pre-combusted glass beads and pre-combusted glass fiber filters at both ends.

217   Two extraction cycles were performed per sample applying a static pressure of 1500 psi and

218   a temperature of 80 °C for 5 min after a heating phase of 5 min. The flush volume was 50 %

219   of the 34 ml cell size with a purging time of 100 s.

220   Extracts were further purified (addition of activated Cu for sulfur and anhydrous Na_2SO_4 for

221   water removal) and then separated into a neutral and an acid fraction using BondElut

222   cartridges (bonded phase NH_2, Varian), eluting with dichloromethane:isopropanol (2:1) for

223   the neutral and methyl *tert*-butyl ether with 4 % acetic acid for the acid fraction according to

224   the method described by van Dongen et al. (2008a). The neutral fraction was further

225   separated into a polar and a non-polar fraction with an Al_2O_3 column. For each of the three

226   compound classes *n*-alkanes (neutral non-polar fraction), *n*-alkanols (neutral polar fraction)

227   and *n*-alkanoic acids (acid fraction) ~10 mg of one internal standard, d_{50}-tetracosane, 2-

228   hexadecanol and d_{39}-eicosanoic acid respectively, were added to the sediment samples prior

229   to extraction. All fractions were then analyzed on a GC–MS (Agilent) using the same column

230   and temperature program as for the CuO products. The polar and acid fractions were

231   derivatized with BSTFA + 1 % TMCS prior to analysis. Quantification was performed using a

232   5-point calibration curve with commercially available standards. Here, we only report data for

233   high-molecular weight (HMW) *n*-alkanes and *n*-alkanoic acids, where HMW refers to carbon

234   chain-lengths of ≥ 23 for *n*-alkanes and ≥ 24 for *n*-alkanoic acids.

3 Results and Discussion

The fate of permafrost-released terrigenous organic carbon (TerrOC) across the Laptev Sea shelf is controlled by competing processes. Degradation and sorting, as well as replacement of TerrOC by autochthonous marine organic matter all co-occur to varying degrees during cross-shelf transport. To disentangle their effects on the fate of permafrost-released TerrOC we first report changes in bulk sediment and OC properties and then focus on differences on the molecular level.

3.1 Characterization of the transect on a bulk level

Bulk total organic carbon (TOC) concentrations decreased across the shelf with highest values (~2 %) at shallow water depths and lowest values on the shelf edge (~0.8 %); at high water depths (> 2000 m) concentrations were slightly higher (~1 %). TOC values and the general pattern were in accordance with previous data from the Laptev Sea (Semiletov et al., 2005; Shakhova et al., 2015; Stein and Fahl, 2004; Vonk et al., 2012) and within the same range of those measured for the North American Arctic margin (Goni et al., 2013). Normalizing TOC concentrations to the mineral-specific surface area (SA) helps to understand the influence of physical sorting and preferential deposition on the observed TOC trends since SA is correlated to the sediment grain size to a first order approximation. To test if the mineral surface area is altered by the input of autochthonous organisms with siliceous or carbonaceous skeleton (e.g. silicoflagellates/diatoms or foraminifera/shells respectively), the mineral composition of the sediments was examined by X-ray fluorescence analysis. There were no apparent trends with water depth for either SiO_2/Al_2O_3 or CaO/Al_2O_3; therefore, marine production is not expected to have a measureable effect and SA can thus be regarded as a conservative parameter. This was also confirmed by low biogenic silica concentrations for the Laptev Sea reported earlier (< 1.4 %, Mammone, 1998). The relationship between TOC and SA has been widely studied on continental margins (e.g. Blair and Aller, 2012; Keil et al., 1994; Mayer, 1994). The TOC/SA ratios of typical river suspended sediments range between 0.4 and 1 mg m^{-2} (Mayer, 1994). TOC/SA ratios > 1

263   mg m^{-2} have been found in areas with high TOC supply (e.g. river outlets) and where the

264   deposited organic matter had spent little time under oxic conditions (short oxygen exposure

265   time, OET) (Mayer et al., 2002). Ratios < 0.4 mg m^{-2} generally correspond to sediments from

266   deeper parts of the ocean and long OETs (e.g. Aller and Blair, 2006). Accordingly, the

267   TOC/SA values along the Laptev Sea transect displayed a strong decrease from 2.2 and 1.7

268   mg m^{-2} close to the Lena River delta (water depths of 11 and 7 m, respectively) to about 0.3

269   mg m^{-2} at water depths greater than 2000 m (Fig. 2A), proposing extensive TOC loss during

270   cross-shelf transport.

271   Bulk TOC isotopes have been broadly used to distinguish between organic matter sources.

272   Radiocarbon isotopes (^{14}C) convey information about the age of organic material, with

273   younger OC having higher Δ^{14}C values. Marine organic matter produced primarily from CO_2

274   is expected to have modern ^{14}C signatures, whereas permafrost-derived TerrOC has aged

275   both on land and during transport and has thus more depleted ^{14}C values. The Δ^{14}C values

276   for our Laptev Sea transect were generally low (< -280 ‰, Fig. 2B), suggesting a significant

277   input of pre-aged TerrOC (as in Vonk et al., 2012). Bulk TOC showed less depleted Δ^{14}C

278   signatures with increasing distance from land on the shelf (from about -500 ‰ to about -340

279   ‰ on the outer shelf, Fig. 2B), reflecting a dilution of older TerrOC with younger marine

280   material. On the slope and rise, however, Δ^{14}C values decreased again to about -410 ‰.

281   This difference may be a result of ageing during lateral transport and/or after deposition due

282   to lower accumulation rates on slope and rise. The range between -340 ‰ and -410 ‰

283   corresponds to a Δ^{14}C age difference of about 900 years; however, the depositional age

284   differences between shelf and slope samples were estimated to be less than 80 years (see

285   Section 2.2). Ageing after burial alone does therefore not explain the difference in Δ^{14}C. Keil

286   et al. (2004) estimated a lateral transport time of 1800 years across the Washington margin

287   (158 km) from Δ^{14}C data of bulk OC in surface sediments. For the > 200 km distance

288   between mid-shelf and rise a bulk ageing of 900 years does therefore not seem

289   unreasonable, particularly since the Washington margin, as opposed to the Laptev Sea shelf,

290   is an active margin. The value from Keil et al. (2004) may therefore be regarded as a lower

291 boundary. It has to be taken into account, however, that mainly the TerrOC fraction of the

292 bulk OC is subject to such protracted lateral transport. Transport times would thus have to be

293 significantly higher in order to explain this age difference for the entire bulk OC. One

294 indication supporting this hypothesis of protracted lateral transport of TerrOC is the

295 degradation status of TerrOC at the deep stations. All molecular degradation proxies point

296 towards highly reworked material (see Section 3.3), suggesting that only the most refractory

297 TerrOC fraction is found at great water depths off the continental margin. Alternatively, the

298 lower Δ^{14}C values at high water depths may be the consequence of more effective

299 degradation of marine organic matter throughout the water column, resulting in a

300 comparatively lower input of young autochthonous material. However, this latter scenario is

301 not supported by the stable carbon isotopic signature, as values for δ^{13}C increase from about

302 -24.3 ‰ on the mid-shelf to about -22.5 ‰, suggesting a higher fraction of marine organic

303 matter for the deep stations.

304 For stable carbon isotopes (^{13}C), terrigenous sources are generally more depleted than

305 marine organic matter (Fry and Sherr, 1984). In this study, values for δ^{13}C of TOC ranged

306 between -26.5 ‰ and -22.3 ‰. The trend towards more enriched TOC with increasing

307 distance from the coast (Fig. 2B) can be explained by a growing proportion of marine organic

308 matter. However, the δ^{13}C signature of the marine source appeared to be heavier than typical

309 marine planktonic material in that region (-26.7 ± 1.2 ‰, Panova et al., 2015; -24 ± 3 ‰,

310 Vonk et al., 2012, and citations therein). One possible explanation for this discrepancy is an

311 underestimated influence of ice algae that were reported to have highly enriched δ^{13}C values

312 between -15 to -18 ‰ (Schubert and Calvert, 2001). Significant seafloor deposition of ice

313 algal biomass has been observed previously for the Arctic basins (Boetius et al., 2013).

314 Another option would be a more refractory, isotopically-enriched marine endmember (-21.2

315 ‰) as suggested by Magen et al. (2010). They argue that lighter isotopes are preferentially

316 consumed by bacteria, which in turn enriches the remaining marine organic matter. Following

317 their reasoning, the more enriched values observed for this transect may be interpreted as

318 an increasing proportion of refractory marine organic matter.

319   Winterfeld et al. (2015b) analyzed surface water particulate organic carbon (POC) in the

320   Lena River delta and found a mean $\delta^{13}C$ of -29.6 ± 1.5 ‰. Karlsson et al. (2011) reported

321   similarly depleted $\delta^{13}C$ values for POC from the Buor-Khaya Bay (-29.0 ± 2.0 ‰), while their

322   mean value for sedimentary OC for the same stations was significantly more enriched (-25.9

323   ± 0.4 ‰) and agreed well with our data for the shallow stations (-26.2 ± 0.3 ‰, stations YS-

324   13, YS-14 and TB-46). Lena River POC $\delta^{13}C$ values from high-discharge periods agree well

325   with the more enriched values we found for the shallow stations (Rachold and Hubberten,

326   1998). Stein and Fahl (2004), Semiletov et al. (2011, 2012) and Vonk et al. (2012) presented

327   similar $\delta^{13}C$ ranges and trends for sediments from parts of the Laptev Sea as is reported in

328   the current study for the entire width of the Laptev Sea shelf. For the Arctic Amerasian

329   Continental shelf, Naidu et al. (2000) reported contrasts in absolute $\delta^{13}C$ values comparing

330   surface sediment samples from different regions, but all commonly displayed an increasing

331   trend for $\delta^{13}C$ values across the shelf, suggesting a growing fraction of marine organic matter

332   with increasing distance from the coast.

333   Combining TOC/SA ratios with stable isotope signatures ($\delta^{13}C$) may serve to disentangle two

334   different processes, which occur synchronously during cross-shelf transport (as in Keil et al.

335   1997a): 1.) The net loss of TerrOC and 2.) the replacement of TerrOC with autochthonous

336   marine OC. Net loss of TerrOC, caused by either degradation or hydrodynamic sorting during

337   transport, has been quantified previously using TOC/SA ratios (e.g. Aller and Blair, 2006; Keil

338   et al., 1997a). The carrying-capacity of inorganic particles for OC is assumed to be a function

339   of the SA (Mayer, 1994); a decrease in TOC/SA values can therefore be regarded as TOC

340   net loss.

341   Replacement of TerrOC with autochthonous marine OC does not change this ratio. But since

342   marine OC is known to be isotopically enriched in $\delta^{13}C$ over TerrOC, this process is recorded

343   by an increasing isotopic signature. Along the Laptev Sea transect, both processes seemed

344   to play an important role (Fig. 2C). High TOC/SA values close to the Lena River decreased

345   sharply outbound in the nearshore regime, pointing to extensive net loss, while the increase

346   in $\delta^{13}C$ values was minor in this area. Once TOC/SA ratios were < 0.8 mg m^{-2} (water depths

347 > 20 m), the isotopic changes and thus the replacement of TerrOC with marine OC became

348 increasingly important. Similar trends were observed for the Amazon River delta (Keil et al.,

349 1997b).

350 However, the TOC/SA trend in the shallower sediments is likely driven by both degradation

351 of OC bound to the mineral matrix during cross-shelf transport and sorting of vascular plant

352 fragments that are retained in the inner shelf. A recent study (Tesi et al., 2016) has shown

353 that ~50 % of the total OC pool in the inner Laptev shelf surface sediments exists in the form

354 of large vascular plant fragments. They are trapped close to the coast due to their size and

355 resulting settling (Stoke's law), while the OC bound to the fine mineral matrix is more buoyant

356 and transported offshore towards deeper waters.

357

358 3.2 Molecular indicators of organic matter sources

359 3.2.1   Biomarker distributions

360 The abundances of different source-diagnostic molecular proxies have been extensively

361 investigated to elucidate complex carbon-cycling mechanisms. In this study, a biomarker

362 suite of CuO oxidation products and solvent-extractable lipids was analyzed in order to gain

363 more insights on TerrOC sources and degradation status along the Laptev Sea transect. All

364 biomarker concentrations were normalized to the sediment-specific surface area (SA)

365 instead of OC content to avoid the signals being overshadowed by other carbon pools. As

366 shown by the lack of water-depth-related changes in the mineral composition (Section 3.1),

367 mineral-matrix dilution by biogenic material is negligible.

368 Lignin-derived phenols have been widely used to trace TerrOC in the marine environment

369 (e.g. Ertel and Hedges, 1984; Goñi and Hedges, 1995; Hedges and Mann, 1979). The lignin

370 macro-molecule is only synthesized in vascular plants (and certain seaweed species that are

371 not existing in the study area) to render stability to the cell walls. Lignin-derived phenols are

372 typically grouped by phenol type (V: vanillyl phenols, i.e. vanillin, acetovanillone, and vanillic

373 acid; S: syringyl phenols, i.e. syringaldehyde, aceto syringone, and syringic acid; C: cinnamyl

374 phenols, i.e. p-coumaric and ferulic acids). Total lignin refers to the sum of the three groups.

375 Across the shelf, lignin loadings decreased substantially with increasing distance from the

376 coast/water depth (45 μg m^{-2} close to the coast, 0.43 ± 0.09 μg m^{-2} for the deep stations; loss

377 of 99.1 ± 0.2 %, Fig. 3A).

378 Cutin-derived hydroxy fatty acids are another compound class obtained from CuO oxidation,

379 which have been used in parallel with lignin phenols (e.g. Goñi et al., 2000; Prahl et al.,

380 1994). They are mainly associated with the soft tissues of vascular plants such as leaves and

381 needles. Cutin acid loadings displayed a similar trend as lignin phenols (11 μg m^{-2} close to

382 the coast, 0.061 ± 0.010 μg m^{-2} for the deep stations; loss of 99.4 ± 0.1 %, Fig. 3A).

383 Similar values and sharp declines with increasing distance from the coast for lignin and cutin

384 have been observed for the whole East Siberian Arctic Shelf (ESAS) (Tesi et al., 2014) (Fig.

385 4 for comparison of lignin phenol concentrations with literature values for different Arctic

386 margins). A recent study (Winterfeld et al., 2015a) for the Buor-Khaya Bay (5.8-17 m water

387 depth) reported lignin phenol concentrations on the same order of magnitude, up to 40 %

388 higher for the shallowest samples, and decreasing with increasing depth. For the Beaufort

389 Sea shelf, Goñi et al. (2000) found a less drastic decline in lignin phenols and cutin acids

390 going from 5 m water depth to 210 m, which likely reflected both lower concentrations in the

391 shallow waters (factor of ~2), and a narrower and steeper shelf. Lignin phenols were also

392 higher at greater water depths than on the ESAS. This may reflect the differences in

393 bathymetry: since the Beaufort Sea shelf is not as wide as, but steeper than, the ESAS,

394 lateral transport is possibly faster, leaving less time for organic matter to be degraded along

395 the way. A comparison between different shelf-slope systems across the North American

396 Arctic margin (Goni et al., 2013) revealed very low lignin and cutin concentrations for the

397 Canadian Archipelago, Lancaster Sound and Davis Strait, whereas both concentrations and

398 trends with water depth for the Beaufort Sea, Chuckchi Sea and Bering Sea were similar to

399 the results from this study. An exception to these patterns was Barrow Canyon, where at

400 water depths of > 2000 m lignin and cutin concentrations were as high as the ones observed

401 close to the Lena River delta, pointing to efficient rapid TerrOC transfer with comparably

402 short oxygen exposure times through this active canyon (Goni et al., 2013) (Fig. 4 and Fig.

403 S1).

404 Solvent extractable high-molecular weight (HMW) *n*-alkanes and *n*-alkanoic acids make up

405 the major part of epicuticular leaf waxes (Eglinton and Hamilton, 1967) and have been

406 broadly employed as TerrOC biomarkers (for the Arctic Ocean e.g. van Dongen et al., 2008;

407 Yunker et al., 1995, 2005). HMW wax lipids in this study also presented a decreasing trend

408 with increasing water depth/distance from the coast, but to a lesser extent than lignin phenols

409 or cutin acids (HMW *n*-alkanes: 1.1 µg m^{-2} close to the coast, 0.12 ± 0.02 µg m^{-2} for the deep

410 stations; HMW *n*-alkanoic acids: 12 µg m^{-2} close to the coast, 0.42 ± 0.29 µg m^{-2} for the deep

411 stations; loss of 89 ± 2 % and 96 ± 3 %, respectively, Fig. 3B).

412 Previous studies in the same area reported similar lipid biomarkers concentrations, which

413 confirm the magnitude of the decreasing trends with increasing water depth (Karlsson et al.,

414 2011; Vonk et al., 2010) (Fig. S1). HMW *n*-alkane concentrations in the Beaufort and the

415 Chuckchi Sea (Belicka et al., 2004; Yunker et al., 1993) are in accordance with the ones

416 measured on the ESAS, but the shallowest sample on the Beaufort Shelf is ~2 times lower

417 than the shallow ESAS samples (Fig. S1). This might imply that sediments transported by the

418 Mackenzie River to the Beaufort Shelf have lower TerrOC concentrations than Lena River

419 transported sediments. For the Mackenzie Shelf, Goñi et al. (2000) used lignin phenols and

420 cutin acids to estimate a terrigenous δ^{13}C endmember and therewith derived a terrigenous

421 contribution of almost 80 % for the shallowest sediments, while rough estimates from C/N

422 and δ^{13}C data suggested that TerrOC made up only 30-50 % of the organic carbon

423 (Macdonald et al., 2004). For the Lena Delta, source apportionment calculations using δ^{13}C

424 and Δ^{14}C data attributed up to 83 % of the organic carbon to terrigenous sources (Vonk et al.,

425 2012).

426 All TerrOC biomarker loadings displayed a strong decrease across the shelf, but their relative

427 losses differ substantially between compound classes (Fig. 3C). These findings agree with

428 previous results for the ESAS (Tesi et al., 2014), where similar differences between

429 biomarkers were reported. A somewhat larger decrease was observed for lignin than for

430   cutin, in contrast to this study. The different extents of biomarker losses for the different

431   compound classes may either be attributed to preferential degradation of lignin phenols and

432   cutin acids, implying that they are more labile than HMW *n*-alkanes and *n*-alkanoic acids, or

433   sorting during transport, suggesting that they are associated with a sediment fraction that is

434   hydraulically more retained and carried less efficiently to the outer shelf/slope. A recent study

435   (Tesi et al., 2016) aimed to disentangle these two processes by analyzing different fractions

436   of bulk surface sediments from three transects (yet with only three stations each) acrossthe

437   ESAS. The fractions were separated according to density ($1.8 \, g \, cm^{-3}$ cutoff), size (>63 µm,

438   38-63 µm, < 38 µm) and settling velocity ($1 \, m \, d^{-1}$ cutoff). The highest lignin phenol

439   abundance was found in low-density plant fragments ($26\text{-}55 \, mg \, g^{-1}$ OC). These large

440   particles have a higher settling velocity (Stokes' law) and are therefore hydraulically retained

441   close to the coast. Cutin acids and plant wax lipids were mainly associated with the high-

442   density fine ($< 38 \, µm, > 1 \, m \, d^{-1}$) and ultrafine ($< 38 \, µm, < 1 \, m \, d^{-1}$) mineral fractions. Within

443   the fine and ultrafine fractions, which made up about 95 % of the organic carbon on the outer

444   shelf, they found drastic losses of all biomarkers with increasing distance from the coast,

445   which they attributed to degradation during the protracted cross-shelf transport. Relative

446   decreases appeared to depend on the number of functional groups of the compound class:

447   98 ± 1 % for lignin phenols, 97 ± 1 % for cutin acids, 96 ± 1 % for HMW *n*-alkanoic acids and

448   89 ± 4 % for HMW *n*-alkanes. According to that study, the steep cross-shelf gradients

449   observed here for lignin phenols can be attributed to both hydrodynamic sorting close to the

450   coast and degradation during transport. From the data in the current study alone, the two

451   processes occurring in parallel - degradation and sorting during cross-shelf transport - cannot

452   be disentangled. However, using the data from (Tesi et al., 2016), we can make a rough

453   correction for the sorting part to derive an estimate of the net extent of degradation. For the

454   shallowest station in their study (same as here, TB-46), about 75 % of the lignin phenols

455   were associated with the low density fraction that was retained close to the coast. If we thus

456   assume only 25 %, i.e. 11 of the 45 $µg \, m^{-2}$ to be associated with the fine fraction that is

457   actually transported across the shelf, we obtain a reduction by 96 ± 1 % that can be

458 attributed to degradation (compared to 99.1 % net loss). These results agree with the values

459 presented in (Tesi et al., 2016). For the other compounds analyzed 55-74 % are associated

460 with the fine fraction even for the shallowest station and they therefore experience sorting to

461 a lesser extent.

462 Degradation after burial is assumed to play only a minor role. Differences in sedimentation

463 ages are expected to be small (Section 2.1) and a study on centennial-scale sediment cores

464 from the East Siberian Sea (Bröder et al., 2016) detected no significant TerrOC degradation

465 (as recorded by biomarker loss) with increasing sediment depth. Also in that study, lignin

466 phenol and cutin acid loadings were on average 20 times higher on the inner than on the

467 outer shelf, whereas for HMW *n*-alkanoic acids and *n*-alkanes the difference between inner

468 and outer shelf was only a factor of ~3-5. Contrasts between the stations were found to be

469 larger than down-core changes. This may be due to the fact that the cores in that study only

470 encompassed about one century of sedimentation ages, while the protracted cross-shelf

471 transport likely requires much longer timescales.

472

473 3.2.2 Lignin Phenol sources

474 Relative distributions of different lignin phenol classes reveal more information on TerrOC

475 sources since they are specific to different plant types. Syringyl phenols are not produced by

476 gymnosperm (non-flowering) plants; elevated syringyl to vanillyl ratios (i.e. S/V > 1, Hedges

477 and Parker, 1976) are therefore attributed to more lignin phenols from angiosperm

478 (flowering) plants. These ratios have to be handled with care, though, because the

479 preferential degradation of syringyl phenols by white- and brown-rot fungi on land can also

480 alter S/V ratios (Hedges et al., 1988). S/V values for the Laptev Sea transect increased with

481 increasing water depth from ~0.65 for the inner shelf to ~1.0 for the slope/rise sediments

482 (Fig. 5A). This trend can either be explained by preferential degradation of gymnosperm

483 material or sorting during transport. Tesi et al. (2014) measured generally lower values for

484 S/V (ESAS average: 0.47, for only Lena watershed dominated locations: 0.42) recording no

485 trend with water depth (Fig. S1 for comparisons with other studies). Their deepest station

was located at only 69 m water depth, though, whereas in this study sediments from down to 3146 m water depth were analyzed. S/V ratios in Buor-Khaya Bay surface sediments (Winterfeld et al., 2015a) were also lower (0.43 ± 0.02 on average) and displayed no trend with water depth. Within the water depth interval they studied (5.8-17 m), however, the samples analyzed in this study had also quite homogeneous S/V ratios (0.64 ± 0.02). Two sediment cores from the East Siberian Sea (Bröder et al., 2016) showed also lower S/V values (inner shelf surface sediment: 0.62, outer shelf surface sediment: 0.50) displaying no clear trends over time/down-core. For the Beaufort Sea shelf Goñi et al. (2000) detected rather high values (0.54-1.71), which (besides the very high value at 61 m water depth) agree with the data from this study. Other transects across the North American Arctic margin (Goni et al., 2013) had slightly lower S/V ratios with no observed trends with water depth.

The ratio of cinnamyl to vanillyl phenols (C/V) is associated with the relative contributions of woody versus soft material, because only non-woody vascular plants synthesize cinnamyl phenols (Hedges and Mann, 1979a). This ratio admittedly decreases with ongoing degradation (Opsahl and Benner, 1995) and may therefore not be used as an unambiguous source indicator. We observed that C/V values strongly decreased across the Laptev Sea Shelf from ~0.5 (close to the Lena River outlet) to ~0.1 (on the slope/rise, Fig. 5B), which may reflect the preferential degradation of soft tissues. This trend is not likely caused by hydrodynamic sorting, since typically the larger, low-density, woody plant fragments are retained in shallower water, whereas finer material is transported further across the shelf (e.g. Keil et al., 1994; Tesi et al., 2016).

C/V ratios in Buor-Khaya Bay sediments (Winterfeld et al., 2015a) in shallow waters were on average lower and more homogeneous (0.17 ± 0.03) than those measured in this study (0.41 ± 0.12 for the corresponding depth interval) (Fig. S1 for comparisons with other studies). C/V values for the entire ESAS were on average 0.15 (0.14 ± 0.07 for only Lena dominated waters) with no water depth trend (Tesi et al., 2014). In shallow sediment cores from the East Siberian Sea, Bröder et al. (2016) measured C/V ratios of 0.20 (inner shelf) and 0.13 (outer shelf) for the surface sediments with no significant trend over sediment depth. For the

Mackenzie Shelf C/V values ranged between 0.16 and 0.32 and slightly increased with increasing water depth (Goñi et al., 2000). In contrast, in the Bering Sea, Chuckchi Sea, Barrow Canyon, Canadian Archipelago, Lancaster sound and Davis Strait there were no C/V trends observed (Goni et al., 2013), with lower values in the Canadian part (0.10 ± 0.12) and highest values on the Beaufort Sea slope, where values slightly decreased with increasing depth (0.39 ± 0.07).

A comparison to the S/V-C/V signatures of potential Arctic plant end-members (compiled by Amon et al., 2012, and citations therein, Tesi et al., 2014, and Winterfeld et al., 2015a) showed that lignin phenols likely derive from both angio- and gymnosperm soft tissues in the shallower samples, closely matching with willow (*Salix*) tissues measured by Winterfeld et al. (2015a). With increasing water depths, angiosperm wood became the most important source material, while gymnosperm wood, grasses and mosses did not appear to contribute significantly to the overall lignin phenol fingerprint (Fig. 5C). As discussed earlier, this trend may well be a result of preferential degradation and sorting during cross-shelf transport and not derive from actual changes in source material.

3.3 Degradation status of organic matter

During degradation, syringyl and vanillyl phenol aldehydes are oxidized to carboxylic acids of the same phenol group. Increasing Sd/Sl and Vd/Vl ratios can therefore qualitatively indicate ongoing degradation of lignin phenols (Ertel and Hedges, 1984; Hedges et al., 1988). For fresh plant material typical acid-to-aldehyde ratios are around 0.1-0.2 (Hedges et al., 1988). Winterfeld et al. (2015a), however, found values as high as Sd/Sl = 0.80 and Vd/Vl = 0.67 for a moss species (*Aulacomnium turgidum*), Sd/Sl = 0.87 for larch (*Larix*) needles and Sd/Sl = 0.49 Vd/Vl = 0.41 for wild rosemary (*Ledum palustre*). Sedges (*Carex spp.*), dwarf birch (*Betula nana*) and willow (*Salix*) range between Sd/Sl = 0.13-0.24 and Vd/Vl = 0.18-0.23. The ratio of CuO oxidation-derived 3,5-dihydroxybenzoic acid to vanillyl phenols (3,5-Bd/V) also serves as a proxy for degradation as 3,5-Bd is formed during humification likely occurring in soils (Gordon and Goñi, 2004; Hedges et al., 1988; Prahl et al., 1994; Tesi et al.,

542 2014). For this reason, this proxy can trace mineral rich soil organic matter in contrast to

543 vascular plant debris (e.g. Dickens et al., 2007; Prahl et al., 1994) as well as degradation

544 during cross shelf transport (Tesi et al., 2016).

545 Sd/Sl, Vd/Vl and 3,5-Bd/V all increased along the transect, implying more degraded material

546 with increasing residence time in the shelf system (Fig. 6A). There appeared to be no

547 differences between outer shelf/slope and rise, which may indicate that TerrOC on the slope

548 is already highly reworked. In contrast, Tesi et al. (2014) found no correlation between Sd/Sl

549 or Vd/Vl and distance from the coast, while 3,5-Bd/V significantly increased with increasing

550 distance from the coast (Fig. S2 for comparisons with other studies). Sd/Sl values for the

551 Buor-Khaya Bay from Winterfeld et al. (2015a) were slightly higher (1.04 ± 0.24) than

552 samples from the corresponding water depths in this study (0.66 ± 0.15), whereas Vd/Vl

553 values were significantly higher (1.28 ± 0.30 compared to 0.59 ± 0.14). Measurements for the

554 Mackenzie Shelf agreed with the ones in this study (Sd/Sl = 0.81 ± 0.25 compared to 1.01 ±

555 0.33 for the corresponding water depths; Vd/Vl = 0.69 ± 0.14 to 0.86 ± 0.26; 3,5-Bd/V = 0.19

556 ± 0.04 to 0.31 ± 0.15), but did not show a trend with water depth (Goñi et al., 2000).

557 Tesi et al. (2016) observed lower acid/aldehyde ratios for the lignin-rich low-density fraction

558 compared to the other fractions (high-density with different grain sizes and settling velocities)

559 in coastal surface sediments from the ESAS. With increasing distance from the coast, these

560 values increased, whereas for the other fractions there were no apparent trends. These

561 findings were interpreted as relatively fresh lignin in the low-density fraction (rich in large

562 plant fragments) compared to the relatively degraded lignin that had likely experienced

563 leaching and adsorbed to the fine mineral fractions (i.e. mineral bound OC). Bulk 3,5-Bd/V

564 values are potentially affected by both sorting and degradation, as they increased with

565 decreasing particle size (fine and ultrafine fractions had the most degraded signal and are

566 preferentially transported to the outer shelf) and across the shelf in each of the fractions.

567 The carbon preference indices for HMW *n*-alkanes and HMW *n*-alkanoic acids have also

568 been widely applied as degradation proxies for plant waxes in marine sediments (for the

569 ESAS, e.g. van Dongen et al., 2008; Fahl and Stein, 1997; Fernandes and Sicre, 2000; Vonk

570   et al., 2010). It measures the ratio of odd-to-even numbers of carbon chain-lengths of HMW

571   lipids and is based on the preference of odd carbon chain-lengths for HMW *n*-alkanes in

572   fresh plant material (even carbon chain-lengths for HMW *n*-alkanoic acids; Eglinton and

573   Hamilton, 1967). With ongoing degradation this preference is lost and the CPI approaches 1

574   (Bray and Evans, 1961).

575   We observed that the HMW *n*-alkane CPI presented a similar pattern as the lignin phenol

576   based degradation indices. However, the HMW *n*-alkanoic acid CPI did not show as much of

577   a degradation trend (HMW *n*-alkane CPI: ~5.7 close to the coast, ~2.2 for the deep stations;

578   HMW *n*-alkanoic acids: ~5.4 close to the coast, ~4.1 for the deep stations; Fig. 6B). Karlsson

579   et al. (2011) measured lipid CPIs in the Buor-Khaya Bay with 10-80 km distance to the coast

580   and obtained similar results to this ~800 km cross-shelf study, with higher values closer to

581   the river delta (Fig. S2 for comparisons with other studies). Their data appears to have a

582   wider spread, though, which might be due to either the narrower dynamic range. Fahl and

583   Stein (1997) also reported a large range of *n*-alkane CPI values (< 0.2- > 5) for Laptev Sea

584   sediments. Fernandes and Sicre (2000) analyzed sediments from the Kara Sea and from the

585   major rivers discharging into this sea, Ob and Yenisey rivers. In the marine environment and

586   the Ob River, they observed HMW *n*-alkane CPI values between 4.8 and 5.3, similar to those

587   found at shallow water depths in this study. For the Yenisey River and mixing zone, they

588   found higher CPI values, pointing to fresher material being transported there. Vonk et al.

589   (2010) recorded HMW *n*-alkane CPI values for sediments along the East Siberian Sea

590   Kolyma paleoriver transect (across the East Siberian Sea) shelf that decreased from > 7.5 to

591   < 4.0 with increasing distance from the river mouth, overall higher than in this study but

592   confirming the general trend to more degraded material on the outer shelf. Tesi et al. (2016)

593   found HMW *n*-alkanoic acid CPI values to decrease with decreasing particle size with no

594   significant trends across the shelf in all but the low-density fraction, which is largely retained

595   close to the shore. The HMW *n*-alkane CPI values in that study, however, showed no

596   systematical differences between different fractions, but an overall decreasing trend with

597   increasing distance from the coast.

598   When undergoing degradation, HMW *n*-alkanoic acids may also lose their functional groups,

599   turning them into HMW *n*-alkanes (Meyers and Ishiwatari, 1993). The slightly decreasing

600   ratio of HMW *n*-alkanoic acids to *n*-alkanes also hints at more degraded material with

601   increasing water depth, although, due to a rather large variability, this trend is not significant.

602   For the Buor-Khaya Bay surface sediments Karlsson et al. (2011) obtained similar results

603   (0.48-10.7, here 1.1-10.9) with higher values closer to the river delta (Fig. S2 for

604   comparisons with other studies). Along the Kolyma paleoriver transect, Vonk et al. (2010)

605   measured HMW *n*-alkanoic acid to *n*-alkane ratios between 1 and 6 with no clear trend with

606   increasing distance from the river mouth. Tesi et al. (2016) found decreasing values with

607   increasing distance from the coast with no differences between the fractions. Two sediment

608   cores from inner and outer East Siberian Sea recording about one century of sedimentation

609   showed no clear trend in CPI or HMW *n*-alkanoic acid/*n*-alkane towards more degraded

610   TerrOC with increasing sediment depth (Bröder et al., 2016), but displayed a similar

611   difference between inner and outer shelf as seen in this study. This contrasting behavior for

612   cross-shelf and down-core trends may be caused by significantly different timescales for the

613   two processes: about one century in situ/after burial compared to potentially several millennia

614   long lateral transport. Furthermore, the degradation efficiency is likely higher under the oxic

615   conditions prevailing during cross-shelf lateral transport (Keil et al., 2004), than in the anoxic

616   conditions that predominate below a few millimeters of sediments on the ESAS (e.g. Boetius

617   and Damm, 1998). Comparing in situ to transport-related oxygen exposure times on the wide

618   Arctic shelves could potentially resolve the observed discrepancies.

4   Concluding remarks and future research directions

Across the Laptev Sea from the Lena River mouth to the deep sea of the Arctic interior a considerable loss of terrigenous organic matter has been observed on both bulk and molecular level. All terrigenous biomarkers display a massive decline with increasing water depth along this high-resolution transect due to hydrodynamic sorting and degradation during transport. Terrigenous organic matter (TerrOC) seems to be also qualitatively more degraded on the outer shelf, slope and rise compared to inner shelf and coastal areas.

These results corroborate and expand previous findings for the East Siberian Arctic Shelf, showing that the shelf seas in this region function as an active reactor for TerrOC. Since the East Siberian Arctic Shelf belongs to the widest and shallowest continental margins on Earth, cross-shelf transport times and thus the time spent in oxic sediments are expected to be comparatively long. This stands in contrast to e.g. the Mackenzie basin, which is thought to act as a geological sink for organic carbon due to its TerrOC burial (Hilton et al., 2015). For narrower Arctic shelves in general, where transport times can be expected to be much shorter, organic matter transfer towards the deeper basins appears to be much more efficient, with high TerrOC concentrations in surface sediments even at greater water depths (e.g. Barrow Canyon, Goni et al., 2013). It can therefore be assumed that the cross-shelf transport time exerts first-order control over the extent of TerrOC degradation. With ongoing global warming, rising permafrost-derived organic carbon input from river-sediment discharge and coastal erosion is expected to reach the marine environment. It is therefore crucial to better constrain cross-shelf transport times in order to determine a TerrOC degradation rate and thereby contribute to quantifying potential carbon-climate feedbacks.

Acknowledgements

We thank crew and personnel of the IB *ODEN*, the RV *Yakob Smirnitskyi* and the *TB0012*. The SWERUS-C3 and the International Siberian Shelf Study 2008 (ISSS-08) expeditions were supported by the Knut and Alice Wallenberg Foundation, Headquarters of the Far

646 Eastern Branch of the Russian Academy of Sciences, the Swedish Research Council (VR

647 Contract No. 621-2004-4039, 621-2007-4631 and 621-2013-5297), the US National Oceanic

648 and Atmospheric Administration (OAR Climate Program Office, NA08OAR4600758/Siberian

649 Shelf Study), the Russian Foundation of Basic Research RFFI (08-05-13572, 08-05-00191-a,

650 and 07-05-00050a), the Swedish Polar Research Secretariat, the Nordic Council of Ministers

651 and the US National Science Foundation (OPP ARC 0909546). L. Bröder also acknowledges

652 financial support from the Climate Research School of the Bolin Climate Research Centre. T.

653 Tesi also acknowledges EU financial support as a Marie Curie fellow (contract no. PIEF-GA-

654 2011-300259), contribution no. 1900 of ISMAR-CNR Sede di Bologna. J.A. Salvadó also

655 acknowledges EU financial support as a Marie Curie grant (FP7-PEOPLE-2012-IEF; project

656 328049). I. Semiletov thanks the Russian Government for financial support (mega-grant

657 #14.Z50.31.0012). O. Dudarev thanks the Russian Science Foundation (grant No. 15-17-

658 20032). Furthermore we would like thank Francien Peterse, Xiaojuan Feng and one

659 anonymous reviewer for their constructive comments, which helped to improve this

660 manuscript.

References

Aller, R. C. and Blair, N. E.: Carbon remineralization in the Amazon-Guianas tropical mobile mudbelt: A sedimentary incinerator, Continental Shelf Research, 26(17-18), 2241–2259, doi:10.1016/j.csr.2006.07.016, 2006.

Amon, R. M. W., Rinehart, A. J., Duan, S., Louchouarn, P., Prokushkin, A., Guggenberger, G., Bauch, D., Stedmon, C., Raymond, P. A., Holmes, R. M., McClelland, J. W., Peterson, B. J., Walker, S. A. and Zhulidov, A. V.: Dissolved organic matter sources in large Arctic rivers, Geochimica et Cosmochimica Acta, 94, 217–237, doi:10.1016/j.gca.2012.07.015, 2012.

Belicka, L. L., Macdonald, R. W., Yunker, M. B. and Harvey, H. R.: The role of depositional regime on carbon transport and preservation in Arctic Ocean sediments, Marine Chemistry, 86(1-2), 65–88, doi:10.1016/j.marchem.2003.12.006, 2004.

Blair, N. E. and Aller, R. C.: The Fate of Terrestrial Organic Carbon in the Marine Environment, Annual Review of Marine Science, 4(1), 401–423, doi:10.1146/annurev-marine-120709-142717, 2012.

Boetius, A. and Damm, E.: Benthic oxygen uptake, hydrolytic potentials and microbial biomass at the Arctic continental slope, Deep-Sea Research Part I: Oceanographic Research Papers, 45(2-3), 239–275, doi:10.1016/S0967-0637(97)00052-6, 1998.

Boetius, A., Albrecht, S., Bakker, K., Bienhold, C., Felden, J., Fernández-Méndez, M., Hendricks, S., Katlein, C., Lalande, C., Krumpen, T., Nicolaus, M., Peeken, I., Rabe, B., Rogacheva, A., Rybakova, E., Somavilla, R. and Wenzhöfer, F.: Export of algal biomass from the melting Arctic sea ice., Science (New York, N.Y.), 339(6126), 1430–2, doi:10.1126/science.1231346, 2013.

Bray, E. . and Evans, E. .: Distribution of n-paraffins as a clue to recognition of source beds, Geochimica et Cosmochimica Acta, 22(1), 2–15, doi:10.1016/0016-7037(61)90069-2, 1961.

Brunauer, S., Emmett, P. H. and Teller, E.: Adsorption of Gases in Multimolecular Layers, Journal of the American Chemical Society, 60(2), 309–319, doi:citeulike-article-id:4074706\rdoi: 10.1021/ja01269a023, 1938.

Bröder, L., Tesi, T., Andersson, A., Eglinton, T. I., Semiletov, I. P., Dudarev, O. V., Roos, P. and Gustafsson, Ö.: Historical records of organic matter supply and degradation status in the East Siberian Sea, Organic Geochemistry, 91, 16–30, doi:10.1016/j.orggeochem.2015.10.008, 2016.

Charkin, A. N., Dudarev, O. V., Semiletov, I. P., Kruhmalev, A. V., Vonk, J. E., Sánchez-García, L., Karlsson, E., Gustafsson, O., Gustafsson, Ö. and Gustafsson, O.: Seasonal and interannual variability of sedimentation and organic matter distribution in the Buor-Khaya Gulf: The primary recipient of input from Lena River and coastal erosion in the southeast Laptev Sea, Biogeosciences, 8(9), 2581–2594, doi:10.5194/bg-8-2581-2011, 2011.

Dethleff, D.: Entrainment and export of Laptev Sea ice sediments, Siberian Arctic, Journal of Geophysical Research C: Oceans, 110(7), 1–17, doi:10.1029/2004JC002740, 2005.

Dethleff, D.: Dense water formation in the Laptev Sea flaw lead, Journal of Geophysical Research: Oceans, 115(12), 1–16, doi:10.1029/2009JC006080, 2010.

Dickens, A. F., Gudeman, J. A., Gélinas, Y., Baldock, J. A., Tinner, W., Hu, F. S. and Hedges, J. I.: Sources and distribution of CuO-derived benzene carboxylic acids in soils and sediments, Organic Geochemistry, 38(8), 1256–1276, doi:10.1016/j.orggeochem.2007.04.004, 2007.

Dmitrenko, I. A., Kirillov, S. A. and Bruno Tremblay, L.: The long-term and interannual variability of summer fresh water storage over the eastern Siberian shelf: Implication for climatic change, Journal of Geophysical Research: Oceans, 113(3), 1–14, doi:10.1029/2007JC004304, 2008.

Eglinton, G. and Hamilton, R. J.: Leaf epicuticular waxes., Science (New York, N.Y.), 156(780), 1322–1335, doi:10.1126/science.156.3780.1322, 1967.

Eicken, H., Reimnitz, E., Alexandrov, V., Martin, T., Kassens, H. and Viehoff, T.: Sea-ice processes in the Laptev Sea and their importance for sediment export, Continental Shelf Research, 17(2), 205–233, doi:10.1016/S0278-4343(96)00024-6, 1997.

Ertel, J. R. and Hedges, J. I.: The lignin component of humic substances: Distribution among soil and sedimentary humic, fulvic, and base-insoluble fractions, Geochimica et Cosmochimica Acta, 48(10), 2065–2074, doi:10.1016/0016-7037(84)90387-9, 1984.

Fahl, K. and Stein, R.: Modern organic carbon deposition in the Laptev Sea and the adjacent continental slope:

Surface water productivity vs. terrigenous input, Organic Geochemistry, 26(5-6), 379–390, doi:10.1016/S0146-6380(97)00007-7, 1997.

Feng, X., Vonk, J. E., van Dongen, B. E., Gustafsson, Ö., Semiletov, I. P., Dudarev, O. V, Wang, Z., Montluçon, D. B., Wacker, L. and Eglinton, T. I.: Differential mobilization of terrestrial carbon pools in Eurasian Arctic river basins., Proceedings of the National Academy of Sciences of the United States of America, 110(35), 14168–73, doi:10.1073/pnas.1307031110, 2013.

Feng, X., Gustafsson, Ö., Holmes, R. M., Vonk, J. E., van Dongen, B. E., Semiletov, I. P., Dudarev, O. V., Yunker, M. B., Macdonald, R. W., Montluçon, D. B. and Eglinton, T. I.: Multi-molecular tracers of terrestrial carbon transfer across the pan-Arctic – Part 1: Comparison of hydrolysable components with plant wax lipids and lignin phenols, Biogeosciences Discussions, 12(6), 4721–4767, doi:10.5194/bgd-12-4721-2015, 2015.

Fernandes, M. B. and Sicre, M. A.: The importance of terrestrial organic carbon inputs on Kara Sea shelves as revealed by n-alkanes, OC and d13C values, in Organic Geochemistry, vol. 31, pp. 363–374., 2000.

Fry, B. and Sherr, E. B.: d13C Measurements as indicators of carbon flow in marine and freshwater ecosystems, Contributions in Marine Science, 27, 13–49, 1984.

Goni, M. A., O'Connor, A. E., Kuzyk, Z. Z., Yunker, M. B., Gobeil, C. and Macdonald, R. W.: Distribution and sources of organic matter in surface marine sediments across the North American Arctic margin, Journal of Geophysical Research-Oceans, 118(9), 4017–4035, doi:10.1002/jgrc.20286, 2013.

Goñi, M. A. and Hedges, J. I.: Sources and reactivities of marine-derived organic matter in coastal sediments as determined by alkaline CuO oxidation, Geochimica et Cosmochimica Acta, 59(14), 2965–2981, doi:10.1016/0016-7037(95)00188-3, 1995.

Goñi, M. A. and Montgomery, S.: Alkaline CuO oxidation with a microwave digestion system: Lignin analyses of geochemical samples, Analytical Chemistry, 72(14), 3116–3121, doi:10.1021/ac991316w, 2000.

Goñi, M. A., Ruttenberg, K. C. and Eglinton, T. I.: A reassessment of the sources and importance of land-derived organic matter in surface sediments from the Gulf of Mexico, Geochimica et Cosmochimica Acta, 62(18), 3055–3075, doi:10.1016/S0016-7037(98)00217-8, 1998.

Goñi, M. A., Yunker, M. B., MacDonald, R. W. and Eglinton, T. I.: Distribution and sources of organic biomarkers in arctic sediments from the Mackenzie River and Beaufort Shelf, Marine Chemistry, 71(1-2), 23–51, doi:10.1016/S0304-4203(00)00037-2, 2000.

Gordeev, V. V.: Fluvial sediment flux to the Arctic Ocean, Geomorphology, 80(1-2), 94–104, doi:10.1016/j.geomorph.2005.09.008, 2006.

Gordon, E. S. and Goñi, M. A.: Controls on the distribution and accumulation of terrigenous organic matter in sediments from the Mississippi and Atchafalaya river margin, Marine Chemistry, 92(1-4 SPEC. ISS.), 331–352, doi:10.1016/j.marchem.2004.06.035, 2004.

Guay, C. K. H., Falkner, K. K., Muench, R. D., Mensch, M., Frank, M. and Bayer, R.: Wind-driven transport for Eurasian Arctic rover discharge, Journal of Geophysical Research, 106(C6), 11469–11480, 2001.

Gustafsson, Ö., Van Dongen, B. E., Vonk, J. E., Dudarev, O. V. and Semiletov, I. P.: Widespread release of old carbon across the Siberian Arctic echoed by its large rivers, Biogeosciences, 8(6), 1737–1743, doi:10.5194/bg-8-1737-2011, 2011.

Günther, F., Overduin, P. P., Sandakov, A. V., Grosse, G. and Grigoriev, M. N.: Short- and long-term thermo-erosion of ice-rich permafrost coasts in the Laptev Sea region, Biogeosciences, 10(6), 4297–4318, doi:10.5194/bg-10-4297-2013, 2013.

Hedges, J. I. and Mann, D. C.: The characterization of plant tissues by their lignin oxidation products, Geochimica et Cosmochimica Acta, 43(11), 1803–1807, doi:10.1016/0016-7037(79)90028-0, 1979a.

Hedges, J. I. and Mann, D. C.: The lignin geochemistry of marine sediments from the southern Washington coast, Geochimica et Cosmochimica Acta, 43(11), 1809–1818, doi:10.1016/0016-7037(79)90029-2, 1979b.

Hedges, J. I. and Parker, P. L.: Land-derived organic matter in surface sediments from the Gulf of Mexico, Geochimica et Cosmochimica Acta, 40, 1019–1029, 1976.

Hedges, J. I., Blanchette, R. A., Weliky, K. and Devol, A. H.: Effects of fungal degradation on the CuO oxidation products of lignin: A controlled laboratory study, Geochimica et Cosmochimica Acta, 52(11), 2717–2726, doi:10.1016/0016-7037(88)90040-3, 1988.

760 Hilton, R. G., Galy, V., Gaillardet, J., Dellinger, M., Bryant, C., O'Regan, M., Gröcke, D. R., Coxall, H., Bouchez, J.
761 and Calmels, D.: Erosion of organic carbon in the Arctic as a geological carbon dioxide sink, Nature, 524(7563),
762 84–87, doi:10.1038/nature14653, 2015.

763 Holmes, R. M., McClelland, J. W., Peterson, B. J., Shiklomanov, I. A., Shiklomanov, A. I., Zhulidov, A. V,
764 Gordeev, V. V and Bobrovitskaya, N. N.: A circumpolar perspective on fluvial sediment flux to the Arctic ocean,
765 Global Biogeochemical Cycles, 16(4), 14–45, doi:10.1029/2001GB001849, 2002.

766 Holmes, R. M., McClelland, J. W., Peterson, B. J., Tank, S. E., Bulygina, E., Eglinton, T. I., Gordeev, V. V.,
767 Gurtovaya, T. Y., Raymond, P. a., Repeta, D. J., Staples, R., Striegl, R. G., Zhulidov, A. V. and Zimov, S. a.:
768 Seasonal and Annual Fluxes of Nutrients and Organic Matter from Large Rivers to the Arctic Ocean and
769 Surrounding Seas, Estuaries and Coasts, 35(2), 369–382, doi:10.1007/s12237-011-9386-6, 2012.

770 Hugelius, G., Strauss, J., Zubrzycki, S., Harden, J. W., Schuur, E. A. G., Ping, C. L., Schirrmeister, L., Grosse, G.,
771 Michaelson, G. J., Koven, C. D., O'Donnell, J. A., Elberling, B., Mishra, U., Camill, P., Yu, Z., Palmtag, J. and
772 Kuhry, P.: Improved estimates show large circumpolar stocks of permafrost carbon while quantifying substantial
773 uncertainty ranges and identifying remaining data gaps, Biogeosciences Discussions, 11(3), 4771–4822,
774 doi:10.5194/bgd-11-4771-2014, 2014.

775 Ivanov, V. V. and Golovin, P. N.: Observations and modeling of dense water cascading from the northwestern
776 Laptev Sea shelf, Journal of Geophysical Research: Oceans, 112(9), 1–15, doi:10.1029/2006JC003882, 2007.

777 Jakobsson, M., Grantz, A., Kristoffersen, Y. and Macnab, R.: Physiography and Bathymetry of the Arctic Ocean,
778 in The Organic Carbon Cycle in the Arctic Ocean, edited by R. Stein and R. W. Macdonald, pp. 1–5., 2004.

779 Karlsson, E. S., Charkin, A., Dudarev, O., Semiletov, I., Vonk, J. E., Sánchez-García, L. and Andersson, A.:
780 Carbon isotopes and lipid biomarker investigation of sources, transport and degradation of terrestrial organic
781 matter in the Buor-Khaya Bay, SE Laptev Sea, Biogeosciences, 8(7), 1865–1879, doi:10.5194/bg-8-1865-2011,
782 2011.

783 Karlsson, E. S., Brüchert, V., Tesi, T., Charkin, a, Dudarev, O., Semiletov, I. and Gustafsson, Ö.: Contrasting
784 regimes for organic matter degradation in the East Siberian Sea and the Laptev Sea assessed through microbial
785 incubations and molecular markers, Marine Chemistry, 170, 11–22, doi:10.1016/j.marchem.2014.12.005, 2014.

786 Keil, R. G., Tsamakis, E., Fuh, C. B., Giddings, J. C. and Hedges, J. I.: Mineralogical and textural controls on the
787 organic composition of coastal marine sediments: Hydrodynamic separation using SPLITT-fractionation,
788 Geochimica et Cosmochimica Acta, 58(2), 879–893, doi:10.1016/0016-7037(94)90512-6, 1994.

789 Keil, R. G., Mayer, L. M., Quay, P. D., Richey, J. E. and Hedges, J. I.: Loss of organic matter from riverine
790 particles in deltas, Geochimica et Cosmochimica Acta, 61(7), 1507–1511, doi:10.1016/S0016-7037(97)00044-6,
791 1997a.

792 Keil, R. G., Tsamakis, E. and Wolf, N.: Relationships between organic carbon preservation and mineral surface
793 area in Amazon fan sediments (Holes 932A and 942A), Proceedings of the Ocean Drilling Program, 155, 531–
794 538 [online] Available from: http://cat.inist.fr/?aModele=afficheN&cpsidt=2169716, 1997b.

795 Keil, R. G., Dickens, A. F., Arnarson, T., Nunn, B. L. and Devol, A. H.: What is the oxygen exposure time of
796 laterally transported organic matter along the Washington margin?, Marine Chemistry, 92(1-4 SPEC. ISS.), 157–
797 165, doi:10.1016/j.marchem.2004.06.024, 2004.

798 Macdonald, R. W., Naidu, A. S., Yunker, M. B. and Gobeil, C.: The Beaufort Sea: distribution, sources, fluxes and
799 burial of organic carbon, in The Organic Carbon Cycle in the Arctic Ocean, edited by R. Stein and R. W.
800 Macdonald, pp. 177–192., 2004.

801 Magen, C., Chaillou, G., Crowe, S. a., Mucci, A., Sundby, B., Gao, A., Makabe, R. and Sasaki, H.: Origin and fate
802 of particulate organic matter in the southern Beaufort Sea - Amundsen Gulf region, Canadian Arctic, Estuarine,
803 Coastal and Shelf Science, 86(1), 31–41, doi:10.1016/j.ecss.2009.09.009, 2010.

804 Mammone, K. A.: Sediment provenance and transport on the Siberian Arctic shelf, Oregon State University.,
805 1998.

806 Mayer, L. M.: Surface area control of organic carbon accumulation in continental shelf sediments, Geochimica et
807 Cosmochimica Acta, 58(4), 1271–1284, doi:10.1016/0016-7037(94)90381-6, 1994.

808 Mayer, L., Benninger, L., Bock, M., DeMaster, D., Roberts, Q. and Martens, C.: Mineral associations and
809 nutritional quality of organic matter in shelf and upper slope sediments off Cape Hatteras, USA: A case of
810 unusually high loadings, Deep-Sea Research Part II: Topical Studies in Oceanography, 49(20), 4587–4597,
811 doi:10.1016/S0967-0645(02)00130-3, 2002.

812 McClelland, J. W., Holmes, R. M., Peterson, B. J., Amon, R., Brabets, T., Cooper, L., Gibson, J., Gordeev, V. V.,
813 Guay, C., Milburn, D., Staples, R., Raymond, P. A., Shiklomanov, I., Stiegl, R., Zhulidov, A., Gurtovaya, T. and
814 Zimov, S.: Development of a Pan-Arctic Database for River Chemistry From Corals to Canyons : The Great
815 Barrier Reef Margin, Program, 89(24), 217–218, doi:10.1029/2006JG000353., 2008.

816 Mercone, D., Thomson, J., Abu-Zied, R. H., Croudace, I. W. and Rohling, E. J.: High-resolution geochemical and
817 micropalaeontological profiling of the most recent eastern Mediterranean sapropel, Marine Geology, 177(1-2), 25–
818 44, doi:10.1016/S0025-3227(01)00122-0, 2001.

819 Meyers, P. A. and Ishiwatari, R.: Lacustrine organic geochemistry-an overview of indicators of organic matter
820 sources and diagenesis in lake sediments, Organic Geochemistry, 20(7), 867–900, doi:10.1016/0146-
821 6380(93)90100-P, 1993.

822 Naidu, A. S., Cooper, L. W., Finney, B. P., Macdonald, R. W., Alexander, C. and Semiletov, I. P.: Organic carbon
823 isotope ratio (d13C) of Arctic Amerasian Continental shelf sediments, International Journal of Earth Sciences,
824 89(3), 522–532, doi:10.1007/s005310000121, 2000.

825 Nieuwenhuize, J., Maas, Y. E. . and Middelburg, J. J.: Rapid analysis of organic carbon and nitrogen in particulate
826 materials, Marine Chemistry, 45(3), 217–224, doi:10.1016/0304-4203(94)90005-1, 1994.

827 Opsahl, S. and Benner, R.: Early diagenesis of vascular plant tissues : Lignin and cutin decomposition and
828 biogeochemical implications, Geochimica et Cosmochimica Acta, 59(23), 4889–4904, 1995.

829 Panova, E., Tesi, T., Pearce, C., Salvadó, J. A., Karlsson, E. S., Kruså, M., Semiletov, I. P. and Gustafsson, Ö.:
830 Geochemical compositional differences of the supramicron plankton-dominated fraction in two regimes of the
831 Marginal Ice Zone (MIZ) of the outer East Siberian Arctic Shelf, in AGU Fall Meeting, p. Conference Abstract
832 C43A–0797., 2015.

833 Pearson, A., Mcnichol, A. P., Schneider, R. J., von Reden, K. F. and Zheng, Y.: Microscale AMS 14C
834 measurement at NOSAMS, Radiocarbon, 40(1), 61–75, 1998.

835 Prahl, F. G., Ertel, J. R., Goni, M. A., Sparrow, M. A. and Eversmeyer, B.: Terrestrial organic carbon contributions
836 to sediments on the Washington margin, Geochimica et Cosmochimica Acta, 58(14), 3035–3048,
837 doi:10.1016/0016-7037(94)90177-5, 1994.

838 Rachold, V. and Hubberten, H. W.: Carbon isotope composition of particulate organic material in east Siberian
839 rivers, Land-Ocean Systems in the Siberian Arctic: Dynamics and History, 223–238, 1998.

840 Rachold, V., Grigoriev, M. N., Are, F. E., Solomon, S., Reimnitz, E., Kassens, H. and Antonow, M.: Coastal
841 erosion vs riverine sediment discharge in the Arctic Shelf seas, International Journal of Earth Sciences, 89(3),
842 450–459, doi:10.1007/s005310000113, 2000.

843 Rachold, V., Eicken, H., Gordeev, V. V, Grigoriev, M. N., Hubberten, H.-W., Lisitzin, A. P., Shevchenko, V. P. and
844 Schirrmeister, L.: Modern Terrigenous Organic Carbon Input to the \textsc{A}rctic \textsc{O}cean, The Organic
845 Carbon Cycle in the Arctic Ocean, 33–55, 2004.

846 Sakshaug, E.: Primary and secondary production in the Arctic Seas, in The Organic Carbon Cycle in the Arctic
847 Ocean, edited by R. Stein and R. W. Macdonald, pp. 57–81., 2004.

848 Salvadó, J. A., Tesi, T., Andersson, A., Ingri, J., Dudarev, O. V., Semiletov, I. P. and Gustafsson, Ö.: Organic
849 carbon remobilized from thawing permafrost is resequestered by reactive iron on the Eurasian Arctic Shelf,
850 Geophysical Research Letters, 42(19), 8122–8130, doi:10.1002/2015GL066058, 2015.

851 Sánchez-García, L., Alling, V., Pugach, S., Vonk, J., Van Dongen, B., Humborg, C., Dudarev, O., Semiletov, I.
852 and Gustafsson, Ö.: Inventories and behavior of particulate organic carbon in the Laptev and East Siberian seas,
853 Global Biogeochemical Cycles, 25(2), 1–13, doi:10.1029/2010GB003862, 2011.

854 Schubert, C. J. and Calvert, S. E.: Nitrogen and carbon isotopic composition of marine and terrestrial organic
855 matter in Arctic Ocean sediments:, Deep Sea Research Part I: Oceanographic Research Papers, 48(3), 789–810,
856 doi:10.1016/S0967-0637(00)00069-8, 2001.

857 Semiletov, I.P., Destruction of the coastal permafrost ground as an important factor in biogeochemistry of the
858 Arctic Shelf waters, Trans. (Doklady) Russian Acad. Sci., 368, 679-682, 1999 (translated into English).

859 Semiletov, I. and Gustafsson, Ö.: East Siberian Shelf Study Alleviates Scarcity of Observations, Eos,
860 Transactions American Geophysical Union, 90(17), 145, doi:10.1029/2009EO170001, 2009.

861 Semiletov, I., Dudarev, O., Luchin, V., Charkin, A., Shin, K. H. and Tanaka, N.: The East Siberian Sea as a

transition zone between Pacific-derived waters and Arctic shelf waters, Geophysical Research Letters, 32(10), 1–5, doi:10.1029/2005GL022490, 2005.

Semiletov, I. P., Pipko, I. I., Shakhova, N. E., Dudarev, O. V., Pugach, S. P., Charkin, A. N., Mcroy, C. P., Kosmach, D. and Gustafsson, Ö.: Carbon transport by the Lena River from its headwaters to the Arctic Ocean, with emphasis on fluvial input of terrestrial particulate organic carbon vs. carbon transport by coastal erosion, Biogeosciences, 8(9), 2407–2426, doi:10.5194/bg-8-2407-2011, 2011.

Semiletov, I. P., Shakhova, N. E., Sergienko, V. I., Pipko, I. I. and Dudarev, O. V: On carbon transport and fate in the East Siberian Arctic land–shelf–atmosphere system, Environmental Research Letters, 7(1), 015201, doi:10.1088/1748-9326/7/1/015201, 2012.

Semiletov, I. P., Shakhova, N. E., Pipko, I. I., Pugach, S. P., Charkin, A. N., Dudarev, O. V., Kosmach, D. A. and Nishino, S.: Space-time dynamics of carbon and environmental parameters related to carbon dioxide emissions in the Buor-Khaya Bay and adjacent part of the Laptev Sea, Biogeosciences, 10(9), 5977–5996, doi:10.5194/bg-10-5977-2013, 2013.

Semiletov, I., Pipko, I., Gustafsson, Ö., Anderson, L. G., Sergienko, V., Pugach, S., Dudarev, O., Charkin, A., Gukov, A., Bröder, L., Andersson, A., Spivak, E. and Shakhova, N.: Acidification of East Siberian Arctic Shelf waters through addition of freshwater and terrestrial carbon, Nature Geoscience, (April), doi:10.1038/NEGO2695, 2016.

Shakhova, N., Semiletov, I., Sergienko, V., Lobkovsky, L., Yusupov, V., Salyuk, A., Salomatin, A., Chernykh, D., Kosmach, D., Panteleev, G., Nicolsky, D., Samarkin, V., Joye, S., Charkin, A., Dudarev, O., Meluzov, A. and Gustafsson, O.: The East Siberian Arctic Shelf: towards further assessment of permafrost-related methane fluxes and role of sea ice., Philosophical transactions. Series A, Mathematical, physical, and engineering sciences, 373(2052), 20140451–, doi:10.1098/rsta.2014.0451, 2015.

Stein, R. and Fahl, K.: Holocene accumulation of organic carbon at the Laptev Sea continental margin (Arctic Ocean): sources, pathways, and sinks, Geo-Marine Letters, 20(1), 27–36, doi:10.1007/s003670000028, 2000.

Stein, R. and Fahl, K.: The Laptev Sea: Distribution, Sources, Variability and Burial of Organic Carbon, in The Organic Carbon Cycle in the Arctic Ocean, edited by R. Stein and R. W. Macdonald, pp. 213–236., 2004.

Stein, R. and Macdonald, R. W., Eds.: The organic carbon cycle in the Arctic Ocean, Springer Verlag., 2004.

Stuvier, M. and Polach, H. A.: Reporting of 14C Data, Radiocarbon, 19(3), 355–363, doi:10.1016/j.forsciint.2010.11.013, 1977.

Syvitski, J. P. M.: Sediment discharge variability in Arctic rivers: Implications for a warmer future, Polar Research, 21(2), 323–330, doi:10.1111/j.1751-8369.2002.tb00087.x, 2002.

Tarnocai, C., Canadell, J. G., Schuur, E. A. G., Kuhry, P., Mazhitova, G. and Zimov, S.: Soil organic carbon pools in the northern circumpolar permafrost region, Global Biogeochemical Cycles, 23(2), 1–11, doi:10.1029/2008GB003327, 2009.

Tesi, T., Semiletov, I., Hugelius, G., Dudarev, O., Kuhry, P. and Gustafsson, Ö.: Composition and fate of terrigenous organic matter along the Arctic land-ocean continuum in East Siberia: Insights from biomarkers and carbon isotopes, Geochimica et Cosmochimica Acta, 133, 235–256, doi:10.1016/j.gca.2014.02.045, 2014.

Tesi, T., Semiletov, I., Dudarev, O., Andersson, A. and Gustafsson, Ö.: Matrix association effects on hydrodynamic sorting and degradation of terrestrial organic matter during cross-shelf transport in the Laptev and East Siberian shelf seas, Journal of Geophysical Research: Biogeosciences, 121(3), 731–752, doi:10.1002/2015JG003067, 2016.

van Dongen, B. E., Semiletov, I., Weijers, J. W. H. and Gustafsson, Ö.: Contrasting lipid biomarker composition of terrestial organic matter exported from across the Eurasian Arctic by the five great Russian Arctic rivers, Global Biogeochemical Cycles, 22(1), 1–14, doi:10.1029/2007GB002974, 2008a.

van Dongen, B. E., Zencak, Z. and Gustafsson, Ö.: Differential transport and degradation of bulk organic carbon and specific terrestrial biomarkers in the surface waters of a sub-arctic brackish bay mixing zone, Marine Chemistry, 112(3-4), 203–214, doi:10.1016/j.marchem.2008.08.002, 2008b.

Vonk, J. E. and Gustafsson, Ö.: Permafrost-carbon complexities, Nature Geoscience, 6(9), 675–676, doi:10.1038/ngeo1937, 2013.

Vonk, J. E., Sánchez-García, L., Semiletov, I., Dudarev, O., Eglinton, T., Andersson, A. and Gustafsson, O.:

912 Molecular and radiocarbon constraints on sources and degradation of terrestrial organic carbon along the Kolyma
913 paleoriver transect, East Siberian Sea, Biogeosciences, 7(10), 3153–3166, doi:10.5194/bg-7-3153-2010, 2010.

914 Vonk, J. E., Sánchez-García, L., van Dongen, B. E., Alling, V., Kosmach, D., Charkin, A., Semiletov, I. P.,
915 Dudarev, O. V., Shakhova, N., Roos, P., Eglinton, T. I., Andersson, A. and Gustafsson, Ö.: Activation of old
916 carbon by erosion of coastal and subsea permafrost in Arctic Siberia, Nature, 489(7414), 137–140,
917 doi:10.1038/nature11392, 2012.

918 Vonk, J. E., Semiletov, I. P., Dudarev, O. V., Eglinton, T. I., Andersson, A., Shakhova, N., Charkin, A., Heim, B.
919 and Gustafsson, Ö.: Preferential burial of permafrost-derived organic carbon in Siberian-Arctic shelf waters,
920 Journal of Geophysical Research: Oceans, 119, 8410–8421, doi:10.1002/2014JC010261.Received, 2014.

921 Wegner, C., Hölemann, J. A., Dmitrenko, I., Kirillov, S. and Kassens, H.: Seasonal variations in Arctic sediment
922 dynamics - Evidence from 1-year records in the Laptev Sea (Siberian Arctic), Global and Planetary Change, 48(1-
923 3 SPEC. ISS.), 126–140, doi:10.1016/j.gloplacha.2004.12.009, 2005.

924 Wegner, C., Bauch, D., Hölemann, J. A., Janout, M. A., Heim, B., Novikhin, A., Kassens, H. and Timokhov, L.:
925 Interannual variability of surface and bottom sediment transport on the Laptev Sea shelf during summer,
926 Biogeosciences, 10(2), 1117–1129, doi:10.5194/bg-10-1117-2013, 2013.

927 Weingartner, T. J., Danielson, S., Sasaki, Y., Pavlov, V. and Kulakov, M.: The Siberian Coastal Current: A wind-
928 and buoyancy-forced Arctic coastal current, Journal of Geophysical Research, 104(C12), 29697,
929 doi:10.1029/1999JC900161, 1999.

930 Wiesenberg, G. L. B., Schwark, L. and Schmidt, M. W. I.: Improved automated extraction and separation
931 procedure for soil lipid analyses, European Journal of Soil Science, 55(2), 349–356, doi:10.1111/j.1351-
932 0754.2004.00601.x, 2004.

933 Winterfeld, M., Goñi, M. A., Just, J., Hefter, J. and Mollenhauer, G.: Characterization of particulate organic matter
934 in the Lena River Delta and adjacent nearshore zone, NE Siberia - Part 2: Lignin-derived phenol compositions,
935 Biogeosciences, 12, 2261–2283, doi:10.5194/bgd-11-14359-2014, 2015a.

936 Winterfeld, M., Laepple, T. and Mollenhauer, G.: Characterization of particulate organic matter in the Lena River
937 delta and adjacent nearshore zone, NE Siberia - Part I: Radiocarbon inventories, Biogeosciences, 12(12), 3769–
938 3788, doi:10.5194/bg-12-3769-2015, 2015b.

939 Yunker, M. B., Macdonald, R. W., Cretney, W. J., Fowler, B. R., Mclaughlin, F. A. and Bay, R. R. B.: Alkane,
940 terpene, and polycyclic aromatic hydrocarbon geochemistry of the Mackenzie River and Mackenzie shelf."
941 Riverine contributions to Beaufort Sea coastal sediment, , 57, 3041–3061, 1993.

942 Yunker, M. B., Macdonald, R. W., Veltkamp, D. J. and Cretney, W. J.: Terrestrial and marine biomarkers in a
943 seasonally ice-covered Arctic estuary — integration of multivariate and biomarker approaches, Marine Chemistry,
944 49(1), 1–50, doi:http://dx.doi.org/10.1016/0304-4203(94)00057-K, 1995.

945 Yunker, M. B., Belicka, L. L., Harvey, H. R. and Macdonald, R. W.: Tracing the inputs and fate of marine and
946 terrigenous organic matter in Arctic Ocean sediments: A multivariate analysis of lipid biomarkers, Deep-Sea
947 Research Part II: Topical Studies in Oceanography, 52(24-26), 3478–3508, doi:10.1016/j.dsr2.2005.09.008, 2005.

948
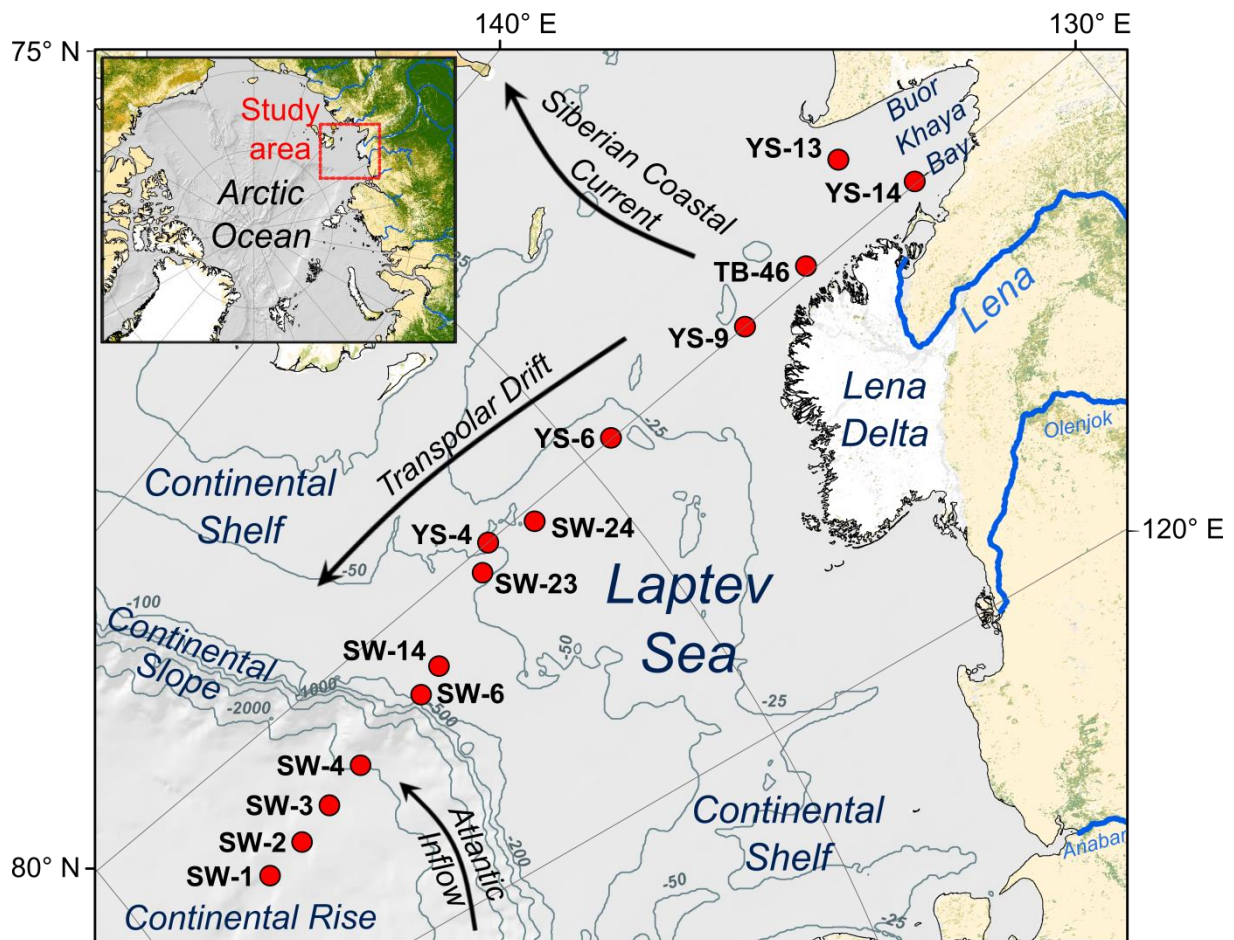
950 Figure 1: Map of the study area in the Laptev Sea. Red filled circles mark the sediment
951 sampling sites. The transect reaches from the Lena River mouth and the Buor-Khaya Bay
952 (water depths ~10 m) across the Laptev Sea Shelf (mean depth ~50 m) to the slope/shelf
953 break and rise (water depths ~3000 m). Arrows show the directions of the prevailing ocean
954 currents.
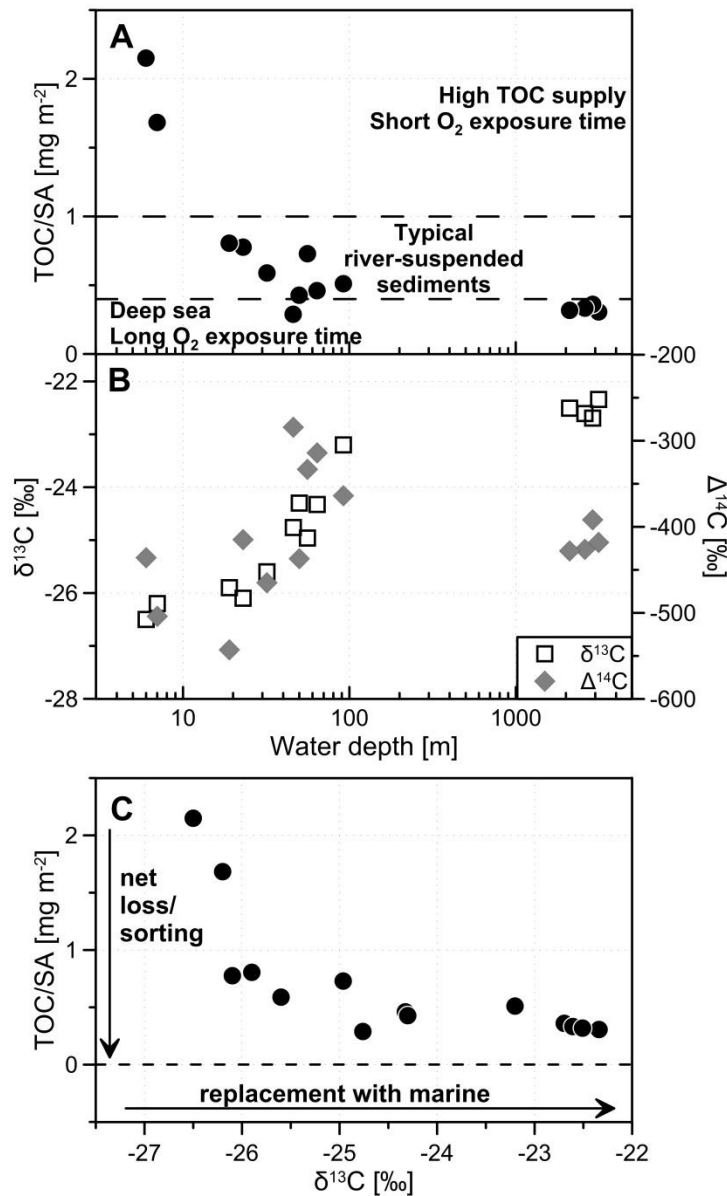
955
956 Figure 2: (A) The ratio of total organic carbon (TOC) to mineral surface area (SA). Typical

957 values for deep sea, river-suspended sediments and high TOC supply are taken from Blair

958 and Aller (2012). (B) The stable carbon isotopic signal (δ^{13}C, open boxes) and the

959 radiocarbon isotopic signal (Δ^{14}C, filled diamonds). (C) The relationship between TOC/SA

960 and δ^{13}C can help to disentangle two processes occurring simultaneously during cross-shelf

961 transport: The net loss (i.e. degradation) or sorting (i.e. hydraulically retaining) of TerrOC

962 leads to a shift towards lower TOC/SA ratios, whereas the replacement/dilution with marine

963 OC shifts the isotopic signature towards higher values.

964
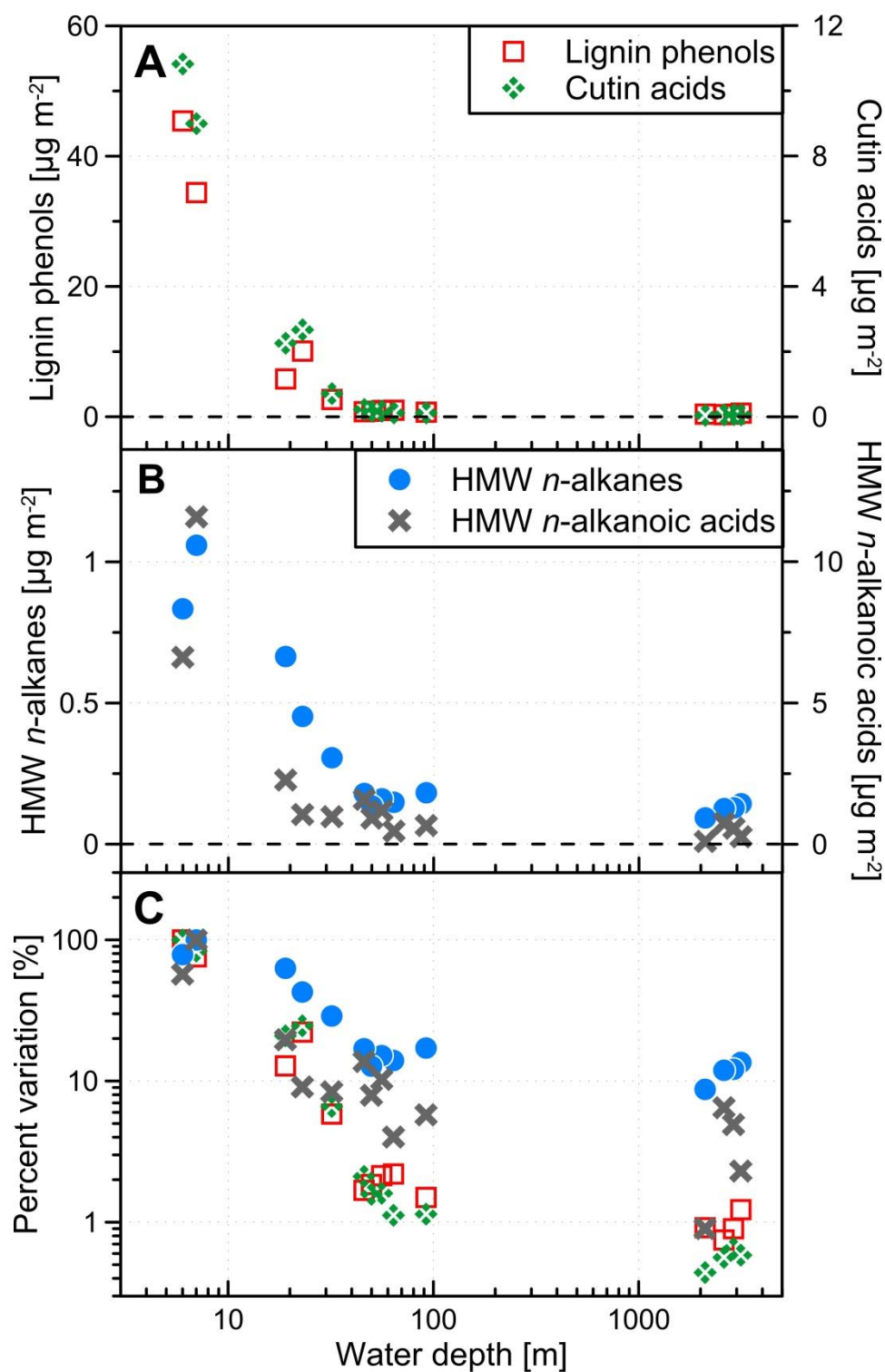
Figure 3: Terrigenous biomarker loadings across the shelf: (A) lignin phenols and cutin acids, (B) HMW *n*-alkanes and HMW *n*-alkanoic acids. (C) Comparison between the different biomarkers along the transect: lignin phenols, cutin acids, HMW *n*-alkanoic acids and *n*-alkanes where each is normalized to respective highest value (corresponding to 100 %).

969
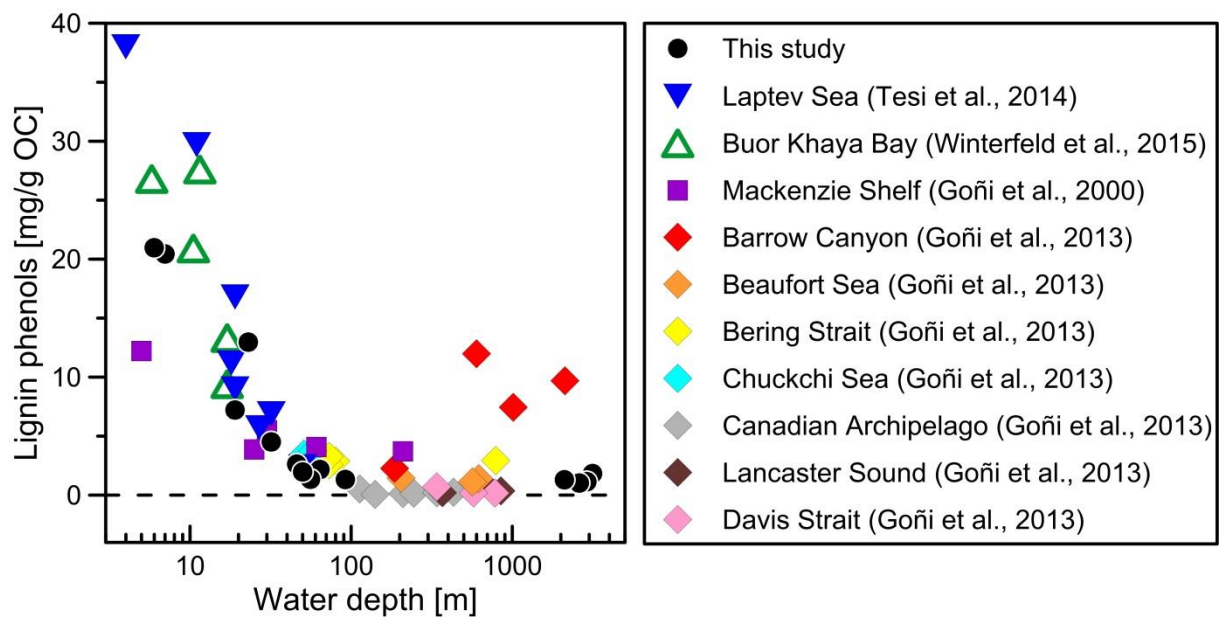
970 Figure 4: A comparison of lignin phenol data from this project to values from published

971 studies around the Arctic Ocean. Similar decreasing trends with increasing water depth are

972 observed for all systems but Barrow Canyon, where elevated lignin phenols concentrations

973 are found even at depth of > 1000 m.

974
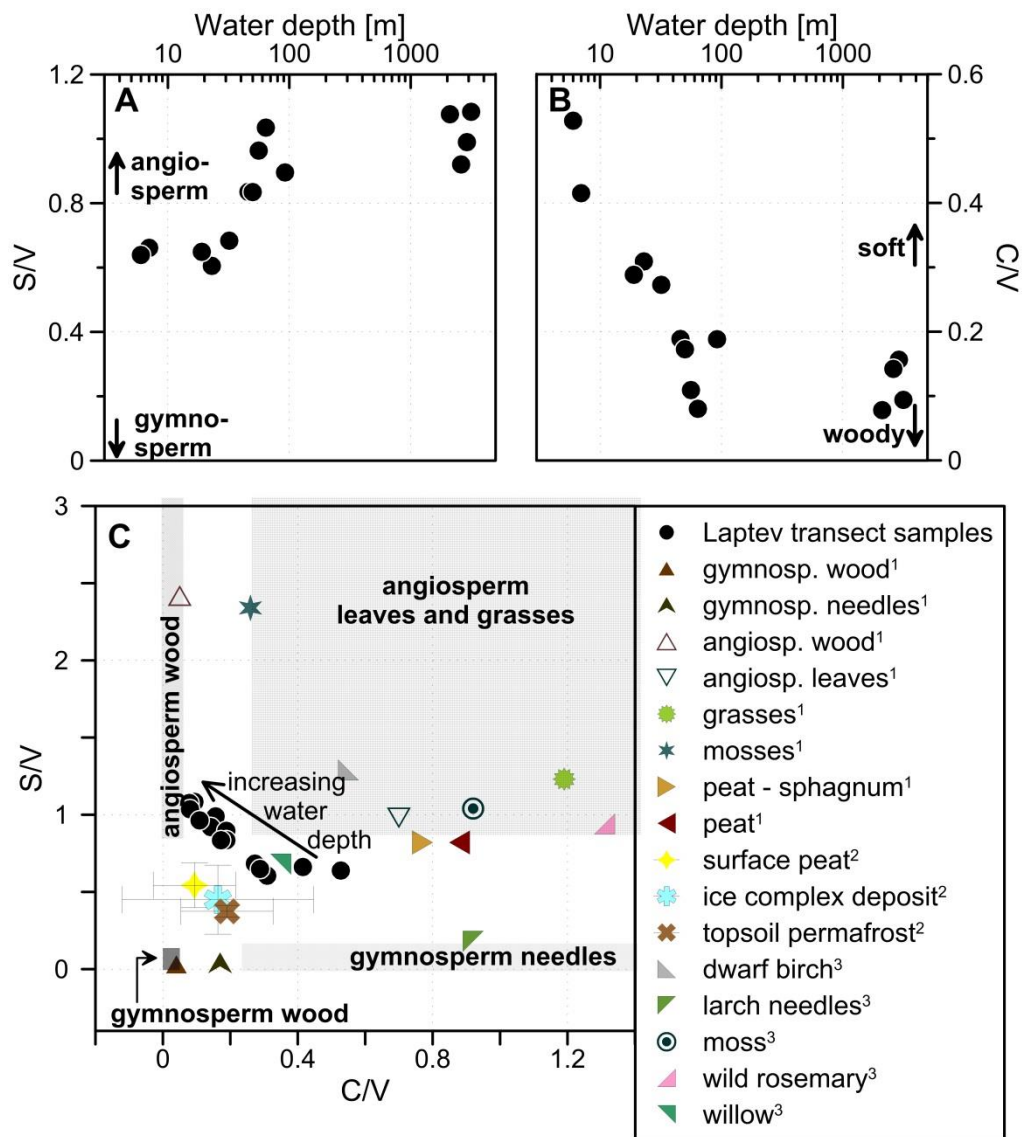
Figure 5: The lignin phenol composition carries source information: (A) an increasing ratio of
syringyl to vanillyl phenols (S/V) suggests relatively more angiosperm material. (B) A
decreasing ratio of cinnamyl to vanillyl phenols (C/V) implies an increasing relative
contribution of woody material compared to soft tissues. (C) Comparison of S/V and C/V with
the end-members for different Arctic plants as compiled from different studies by Amon et al.
(2012, and citations therein, here marked with [1]); ice-complex deposit and topsoil permafrost
as determined by Tesi et al. (2014, here marked with [2]) and more plant species measured by
Winterfeld et al. (2015a, here marked with [3]). The boxes indicate typical ranges of S/V and
C/V for different vascular plant tissues in different locations (e.g. Goñi et al., 2000).

984
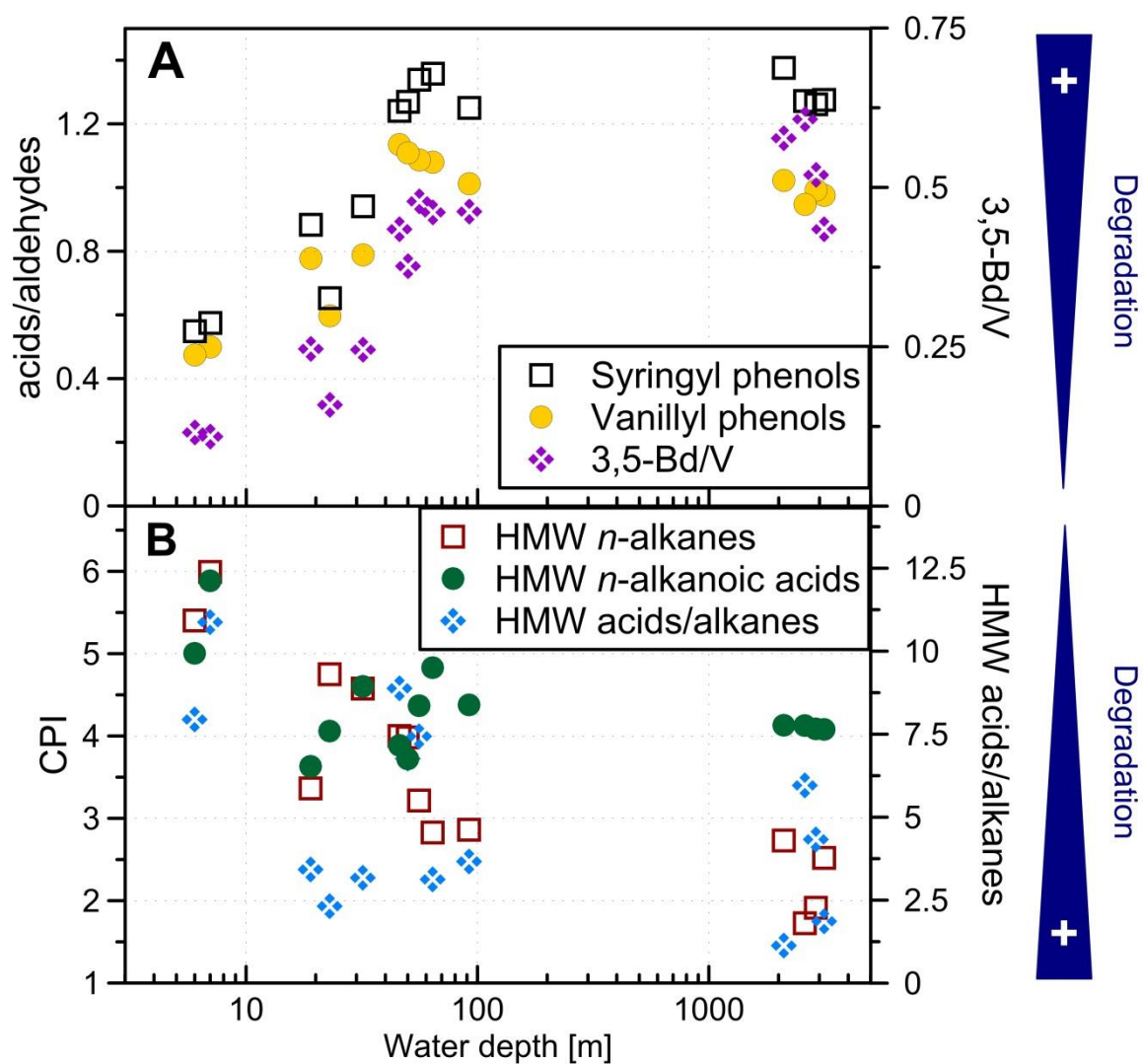
Figure 6: Degradation proxies for TerrOC, blue triangles point toward lower extent of

degradation: (A) CuO-oxidation derived ratios Sd/Sl, Vd/Vl and 3,5-Bd/V. (B) Carbon

preference indices (CPI) of HMW *n*-alkanes and *n*-alkanoic acidsand the ratio of HMW *n*-

alkanoic acids to HMW *n*-alkanes.

989

Table 1: List of surface sediment samples from the Laptev Sea transect

ID	Sample type	Lat	Long	Water depth	OC	SA	$\delta^{13}C$	$\Delta^{14}C$	SiO_2	Al_2O_3	CaO
		° N	° E	m	mg g^{-1}	m^2 g^{-1}	‰	‰	wt %	wt %	wt %
SW-1	0-0.5cm	78.942	125.243	3146	10.4	34.0	-22.3	-418	60.3	16.5	2.4
SW-2	0-0.5cm	78.581	125.607	2900	13.8	38.3	-22.7	-392	57.8	17.2	2.1
SW-3	0-0.5cm	78.238	126.150	2601	10.6	31.8	-22.6	-426	62.1	16.0	1.6
SW-4	0-0.5cm	77.855	126.664	2106	13.2	41.5	-22.5	-428	56.6	17.5	1.3
SW-6	0-1cm	77.142	127.378	92	7.6	14.9	-23.2	-364	72.0	12.6	1.7
SW-14	0-1cm	76.894	127.798	64	8.9	19.4	-24.3	-314	71.3	12.5	1.5
SW-23	0-1cm	76.171	129.333	56	15.8	21.7	-25.0	-333	68.9	13.6	1.4
YS-4	0-1cm	75.987	129.984	50	13.4[a]	31.4	-24.8[a]	-284[a]	63.8	15.1	1.3
SW-24	0-1cm	75.599	129.558	46	10.7	37.0	-24.3	-437	62.5	15.4	1.2
YS-6	0-1cm	74.724	130.016	32	18.6[a]	31.6	-25.6[a]	-465[a]	62.1	16.1	1.3
YS-9	Grab	73.366	129.997	23	13.1[b]	16.9	-26.1[b]	-415[b]	70.8	14.0	1.3
YS-13	0-1cm	71.968	131.701	19	18.9[a]	23.5	-25.9[a]	-543[a]	61.6	17.4	0.8
YS-14	0-1cm	71.630	130.050	7	19.1[a]	11.4	-26.2[a]	-504[a]	69.6	15.0	1.6
TB-46	Grab	72.700	130.180	6	25.8[a]	12.0[c]	-26.5[a]	-436[a]	67.9	15.2	1.8

[a] Data from Vonk et al. (2012); [b] data from Tesi et al. (2016); [c] data from Karlsson et al. (2014).

Table 2: Biomarker results for surface sediment samples from the Laptev Sea transect

ID	Lignin	Cutin	HMW* alkanes	HMW** acids	S/V	C/V	Sd/Sl	Vd/Vl	3,5Bd/V	CPI alk	CPI acids	acids/ alk
	$\mu g\ m^{-2}$	$\mu g\ m^{-2}$	$\mu g\ m^{-2}$	$\mu g\ m^{-2}$								
SW-1	0.56	0.063	0.14	0.27	1.1	0.09	1.3	0.98	0.43	2.5	4.1	1.9
SW-2	0.41	0.070	0.13	0.57	0.99	0.16	1.3	0.99	0.52	1.9	4.1	4.3
SW-3	0.34	0.061	0.13	0.75	0.92	0.14	1.3	0.95	0.61	1.7	4.1	6.0
SW-4	0.42	0.048	0.093	0.10	1.1	0.08	1.4	1.0	0.58	2.7	4.1	1.1
SW-6	0.68	0.12	0.18	0.67	0.90	0.19	1.2	1.0	0.46	2.9	4.4	3.7
SW-14	1.0	0.12	0.15	0.46	1.0	0.08	1.4	1.1	0.46	2.8	4.8	3.1
SW-23	0.97	0.17	0.16	1.2	0.96	0.11	1.3	1.1	0.48	3.2	4.4	7.4
YS-4	0.84	0.17	0.13	0.92	0.83	0.17	1.3	1.1	0.38	4.0	3.7	6.8
SW-24	0.76	0.23	0.18	1.6	0.84	0.19	1.2	1.1	0.43	4.0	3.9	8.9
YS-6	2.7	0.71	0.31	0.97	0.68	0.27	0.94	0.79	0.25	4.6	4.6	3.2
YS-9	10	2.7	0.45	1.1	0.60	0.31	0.65	0.60	0.16	4.7	4.1	2.3
YS-13	5.8	2.3	0.64	2.3	0.65	0.29	0.88	0.78	0.25	3.4	3.6	3.4
YS-14	34	9.0	1.1	12	0.66	0.42	0.57	0.50	0.11	6.0	5.9	11
TB-46	45	11	0.83[d]	6.6[d]	0.64	0.53	0.55	0.47	0.12	5.4[d]	5.0[d]	7.9[d]

995

996   * carbon chain-lengths 23-34; ** carbon chain-lengths 24-30.

997   [d] recalculated data from Karlsson et al. (2011).